TOPICS IN STRUCTURAL DYNAMICS -NONLINEAR UNSTEADY TRANSONIC FLOWS AND MONTE CARLO METHODS IN ACOUSTICS

Final Report
Grant No. NGL 47-005-108

Submitted to:

National Aeronautics and Space Administration
Washington, D. C. 20546

Submitted by:

Dr. John Kenneth Haviland
Professor

RESEARCH LABORATORIES FOR
THE ENGINEERING SCIENCES
SCHOOL OF ENGINEERING AND APPLIED SCIENCE

UNIVERSITY OF VIRGINIA
CHARLOTTESVILLE

Report No. ESS-4022-113-74

February 1974

TOPICS IN STRUCTURAL DYNAMICS
-NONLINEAR UNSTEADY TRANSONIC FLOWS
AND MONTE CARLO METHODS IN ACOUSTICS

Final Report
Grant No. NGL 47-005-108

Submitted to:

National Aeronautics and Space Administration
Washington, D. C. 20546

Submitted by:

Dr. John Kenneth Haviland
Professor

Department of Engineering Science and Systems

RESEARCH LABORATORIES FOR THE ENGINEERING SCIENCES

SCHOOL OF ENGINEERING AND APPLIED SCIENCE

UNIVERSITY OF VIRGINIA

CHARLOTTESVILLE, VIRGINIA

Report No. ESS-4022-113-74
February 1974

Copy No. 1

ABSTRACT

This report covers work on two unrelated tasks. The first was an investigation of the formulation of the equations for non-uniform unsteady flows, by perturbation of an irrotational flow to obtain the linear Green's equation. The resulting integral equation was found to contain a kernel which could be expressed as the solution of the adjoint flow equation, a linear equation for small perturbations, but with non-constant coefficients determined by the steady flow conditions. For the uniform flow case, this kernel was found to limit to the doublet form commonly used in formulating the flutter problem. It is believed that the non-uniform flow effects may prove important in transonic flutter, and that in such cases, the use of doublet type solutions of the wave equation would then prove to be erroneous. The second task covered an initial investigation into the use of the Monte Carlo method for solution of acoustical field problems. Computed results are given for a rectangular room problem, and for a problem involving a circular duct with a source located at the closed end. In both cases, results appear to be within statistical expectations, although statistical deviations were large because computer time was limited. The most severe limitation to further applications of the method is the need for a suitable method to handle acoustical diffraction, as in a shadow zone, or near a window in a room.

LIST OF FIGURES

TABLE OF CONTENTS

INTRODUCTION

Work under this grant started on October 1, 1969 and was terminated on September 30, 1973. The main effort was concentrated on two tasks: (A) Numerical Methods of Solution of Non-Linear Unsteady Transonic Flows, undertaken entirely by the author, and (D) Application of Monte Carlo Methods to Acoustical Analysis, undertaken as a doctoral dissertation by Balakrishna Thanedar, with the author acting as adviser. Two other tasks were briefly worked on, but were abandoned before any appreciable effort had been expended. These were: (B) Dynamic Interaction of Tracked Air Cushion Vehicle and Guideway; and (C) Computer Model for Aircraft Ride Environment Analysis.

Work under task (A) became divided into two major subtasks. The first was continued up to the termination of the project, and consisted of investigations into methods of formulating the nonlinear transonic flow problem. It has resulted in a Note[1] to the AIAA Journal, "The Integral Equation for Small Perturbations of Irrotational Flows", in which it is shown that the Green's Function required for the formulation of the integral equation relating normal flow velocity to local velocity potential is the unit solution of the adjoint wave equation. Hitherto, it has generally been assumed that it is the unit solution of the wave equation.

The second subtask concerned the formulation of the flutter equation in terms of velocity potentials. It was argued that the nonlinear transonic problem might be approached more readily in terms of the velocity potential. However, before this formulation could be used with confidence in the nonlinear solution, it would be necessary to check it against known results for the linear case. A computer program was prepared, using not only the "downwash-velocity potential method" (often called the "integrated potential method") but also introducing the concept of "aerodynamic elements". This effort was transferred to NASA Grant No. NGL-47-005-098 "Numerical Methodology for Flutter Analysis and Optimization of Aircraft Structures" during 1971. It has since resulted in a paper[2] published in the AIAA Journal; "Downwash-Velocity Potential Method for Oscillating Surfaces". Two more papers are planned, and a final report on the work under this grant is in review. The present status of the method is that it has been developed for out-of-plane polygonal elements in subsonic and supersonic flow.

Work under task (D) had its first results in the demonstration of a Monte Carlo solution for a rectangular room. This was presented to the April 1971 meeting of the Acoustical Society, and will be published[3] shortly in their Journal as "Monte Carlo Applications to Acoustical Field Solutions". Since then, a solution for a circular duct was

obtained. Both of these solutions were described in a doctoral dissertation by Thanedar[4], "Monte Carlo Investigation of Transient Acoustic Fields in Partially or Completely Bounded Media".

Discussions of the two tasks are given separately in Parts I and II of this report.

PART I

NUMERICAL METHODS OF SOLUTION OF NONLINEAR UNSTEADY TRANSONIC FLOWS

I.1 DISCUSSION

The aerodynamic disturbances which are transmitted from point to point on an oscillating wing depend, for their velocity, on the local velocity of sound and on the local airflow velocity. It might therefore appear obvious that local variations of the speed of sound would result in appreciable modification of the aerodynamic behavior of the wing when the airflow is locally sonic. Interest in this problem has been spurred by poor agreement between experiment and theory in transonic flows as compared to moderate to good agreement in subsonic and supersonic flows. The nonlinear transonic problem has been studied by a number of authors, generally as a linear perturbation.

Two major considerations spurred the work performed under this grant; (1) that the generally accepted linearized form of the integral equation was open to suspicion, as it seemed to imply that a pressure disturbance on a wing anticipates the local normal flow resulting from a deflection of the surface; and (2) that the downwash velocity potential formulation is a potential building block of any numerical formulation, because the kernel of the integral equation directly relates velocity potential at one point to normal flow velocity

(downwash) at another. In the downwash-pressure formulation, on the other hand, the kernel relates an integral of the wake to infinity behind one point to the normal flow velocity at another.

A tentative approach to the development of a transonic method was formulated as follows:

(a) Develop a subsonic uniform flow method based on the downwash-velocity potential formulation.

(b) Develop the same for the supersonic case.

(c) Develop a ray tracing method to permit calculation of the time lag and attenuation between pairs of points.

(d) Develop a steady flow solution for finite thickness wings. This is needed to provide a medium through which rays can be traced.

(e) Combine into one program. This would perform the following:

(i) Compute local steady state flow velocities and Mach numbers

(ii) Perform ray tracing calculations connecting pairs of points

(iii) Form the aerodynamic matrix by substituting actual attenuation and time lag values, calculated by ray tracing, into kernels of expressions developed from linear equations.

(iv) Use the aerodynamic matrix as appropriate to complete the solution of the problem.

Steps (a) and (b) were initiated under this grant and have since been achieved in separate efforts, as noted in the Introduction. Step (c) has been taken to the point that the correct integral equation has been formulated. The next move requires ray tracing with the adjoint equation, which has not yet been attempted. Steps (d) and (e) have not been initiated.

Different methods of analysis which have been proposed are discussed in the following section, and work on the formulation of the integral equation, as required for step (c), is described in Section I.3.

I.2. REVIEW OF METHODS OF ANALYSIS

Ray Tracing

As will be shown in the following section, the correct formulation for the flow velocity in the normal direction is given by Eq.(I-53). This expression includes the Green's function G, which must satisfy the adjoint wave equation, as expressed by Eq.(I-30). However, it has often been assumed that the Green's Function and the source solution defined by Eq.(I-43) are identical. The precise effect of this assumption is not understood at this time, but, as shown in the next section, they are identical in the uniform flow case, and have the following values

$$G = U(\tau_R) G_R + U(\tau_A) G_A$$

where the subscripts R, A stand for retarded and advanced, respectively, and $U(\chi)$ is a cutoff function which equals unity when χ is real and positive, zero otherwise. Also

$$G_R = - e^{-i\omega\tau_R}/4\pi R$$

$$G_A = - e^{-i\omega\tau_A}/4\pi R$$

where $$R = \sqrt{(x-\xi)^2 + \beta^2(y-\eta)^2 + \beta^2(z-\zeta)^2}$$

The points x, y, z and ξ, η, ζ are the 'receiving' point $\mathcal{R}$ and the 'disturbing point' $\mathcal{P}$, respectively. The terms τ_R, τ_A are the times taken by the retarded and advanced waves, respectively, to go from the disturbing

point to the receiving point, and are given by

$$\tau_R = \{R - M(x-\xi)\} / \beta^2 c$$

$$\tau_A = \{-R - M(x-\xi)\} / \beta^2 c$$

where $\beta^2 = 1 - M^2$

and c = speed of sound.

It is apparent from the above expressions that only the retarded wave arrives at the receiving point in a subsonic flow, and that both waves arrive in supersonic flow only if the receiving point is located in the aft Mach cone from the disturbing point.

An obvious approach to a solution of the nonlinear problem would be to determine values for τ_R, τ_A, R, M, and c appropriate to the actual non-uniform solution. Evaluation of these quantities would require some form of solution of the non-uniform wave equation, possibly by ray tracing.

Several possible ray tracing approaches have been considered, but since it has been determined that rays should be traced with the adjoint equation, as demonstrated in the next section, no firm understanding has been developed of how this ray tracing is to be done.

The approach described here was originally suggested by Andrew and Stenton[5], the idea of determining and

and substituting new values for τ_R and τ_A having been suggested by Landahl[6].

Small Perturbation Methods

A summary by Bland[7] shows that five different approaches to the transonic aerodynamics problem are based on the small disturbance potential equation given by Landahl[8]. Assuming that the velocity potential can be expressed as the sum of a steady and an oscillating part, as in Eq.(I-14), a linear differential equation is derived with variable coefficients. This is also true of Eq.(I-20), but the two equations are different, presumably due to approximations introduced into Landahl's, which is valid only for transonic flows.

Finite-Difference Method

This method has been investigated by Ehlers[9] for the two-dimensional case, with promising results. Within the limitations of computer storage, it should be possible to obtain results by this method, regardless of how the perturbation equation is formulated.

Local Linearization Procedure

This analytical method has been investigated by Stahara and Spreiter[10], and has been developed from methods used for the solution of steady problems.

Layered Medium Analysis

This has been investigated by Revell[11]. The region around the wing is divided into subsonic and supersonic areas,

which are further subdivided into horizontal layers in which local speeds of sound and Mach numbers are assumed to be constant. Linear solutions in each layer are matched at the boundaries to form complete solutions. Numerical results are not yet available.

Lifting Surface Element Method

This has been investigated by Cunningham[12]. The surfaces are divided into smaller elements, each assumed to be in uniform flow, but with a flow condition different to tha adjacent elements. The normal velocity components at collocation points are then calculated much as in many of the variants of Watkins[13] kernel function method, more especially as in the collocation method developed by Cunningham[14], except that the local flow conditions are used in each case.

Modified Sonic Box Method

This method, investigated by Ruo, Yates, and Theisen[15] is a modification of the sonic box method of Rodemich and Andrew[16], in which a transformation is used to replace a nonconstant Mach number by a constant one. A flutter calculation on a delta wing using this method showed the correct trend as thickness was varied.

I-3 THE INTEGRAL EQUATION FOR TRANSONIC FLOWS

Introduction

The correct form of solution of the problem of oscillating airfoils in non-uniform irrotational flow is examined by linear perturbation.

It is shown that the kernel of the integral equation giving the unknown velocity potential perturbation on the surface, as a function of the known normal flow or "downwash" perturbation, is the second derivative of a Green's function. It is also shown that an approximate solution of this function might be sought by reverse ray tracing with the adjoint wave equation, i.e., by starting at the "downwash" point, or "receiving" point, and proceeding towards the "potential perturbation" point or "disturbing" point.

It might appear, intuitively, that the kernel could be obtained from a source solution, in which a ray is traced from the "disturbing point" to the "receiving" point. This is all the more plausible as it corresponds to the method used in the literature[13] to obtain the kernel in the uniform flow case. However, in the latter case, either method would lead to the same result because the wave operator is Hermetian (i.e. its transpose is its adjoint so that its adjoint is also the operator for a reverse flow).

Unfortunately, the non-uniform flow wave operator is not Hermetian, so that the direct ray tracing technique leads to incorrect results for non-uniform flows.

Definitions

Coordinates

$\vec{r}$ = Coordinate Vector of "receiving" or "downwash" point

$\vec{\rho}$ = Coordinate Vector of "sending", "potential perturbation" or "dummy" point

n = Normal coordinate to bounding surface at point $\vec{r}$

u = Normal coordinate to bounding surface at point $\vec{\rho}$

ν = Normal coordinate to one-sided surface S at $\vec{\rho}$

x = Coordinate parallel to the flow

λ = Dummy for x

Symbols

c = local speed of sound

G = Green's function

P = Pressure

p = amplitude of pressure perturbation

$\vec{q}$ = Flow velocity vector

S = One-sided surface

σ = Bounding surface

t = time

$\vec{V}$ = Steady flow velocity vector

υ = Volume bounded by S

Φ, Φ_o = Velocity potential and steady component

ϕ = amplitude of velocity potential perturbation

$\hat{\mu}$ = Unit normal to surface

ρ, ρ_o = Density and steady component

ω = Radial frequency

ψ = Amplitude of pressure potential perturbation

Operators

$\mathcal{L}, \tilde{\mathcal{L}}$ = Wave operator and adjoint

$\mathbb{P}$ = Bilinear concommitant

∇ = Del operator

Δ = Difference across a discontinuity

Subscripts

r, s = Indicate variable of differentiation

A = Airfoil surface, as opposed to wake

L = Lower

U = Upper

Potential Equation for Irrotational Adiabatic Flow

For an irrotational flow, the velocity vector q can be derived from a potential Φ by

$$q = \nabla \Phi \tag{I-1}$$

then

$$\nabla \times q = 0 \tag{I-2}$$

Because the flow is adiabatic, the pressure is a function of density ρ only, so that

$$P = P(\rho) \tag{I-3}$$

and

$$dP/d\rho = c^2(P) \tag{I-4}$$

Writing the continuity equation as

$$\partial \rho / \partial t + \nabla \cdot \rho q = 0 \tag{I-5}$$

and rearranging after substituting from Eq. (4)

$$\frac{1}{\rho} \frac{\partial P}{\partial t} + \frac{1}{\rho} q \cdot \nabla P + c^2 \nabla \cdot q = 0 \tag{I-6}$$

Euler's equation can be written as

$$\frac{\partial \mathbf{q}}{\partial t} + (\mathbf{q}\cdot\nabla)\mathbf{q} + \frac{1}{\rho}\nabla P = 0 \qquad \text{(I-7)}$$

From a theorem on vectors

$$(\mathbf{q}\cdot\nabla)\mathbf{q} = \frac{1}{2}\nabla q^2 - \mathbf{q}\times(\nabla\times\mathbf{q}) \qquad \text{(I-8)}$$

Thus, substituting in Euler's equation, and noting that the last term disappears according to Eq.(2), the following form of Euler's equation results

$$\frac{\partial \mathbf{q}}{\partial t} + \frac{1}{2}\nabla q^2 + \frac{1}{\rho}\nabla p = 0 \qquad \text{(I-9)}$$

But, substituting from Eq.(1), this can be written as

$$\nabla\left(\frac{\partial \Phi}{\partial t} + \frac{1}{2}q^2 + \int\frac{dP}{\rho}\right) = 0 \qquad \text{(I-10)}$$

which can be readily integrated to give a form of Bernoulli's equation

$$\frac{\partial \Phi}{\partial t} + \frac{1}{2}q^2 + \int\frac{dP}{\rho} = f(t) \qquad \text{(I-11)}$$

Now, premultiply Eq.(9) by $\mathbf{q}$, add $\partial/\partial t$ of Eq.(11), and subtract Eq.(6) to obtain

$$\frac{\partial^2 \Phi}{\partial t^2} + \frac{\partial q^2}{\partial t} + \frac{1}{2}\mathbf{q}\cdot\nabla q^2 = c^2\nabla\cdot\mathbf{q} \qquad \text{(I-12)}$$

With a slight rearrangement, and a substitution from Eq.(1), the form given by Garrick[17] results

$$\frac{\partial^2 \Phi}{\partial t^2} + \frac{\partial q^2}{\partial t} + \frac{1}{2}\mathbf{q}\cdot\nabla q^2 = c^2\nabla^2\Phi \qquad \text{(I-13)}$$

Perturbation Equation

The flow is assumed to consist of a steady component with a small harmonic perturbation, so that

$$\Phi = \Phi_o + \phi e^{i\omega t} \tag{I-14}$$

and

$$q = V + \nabla\phi e^{i\omega t} \tag{I-15}$$

where both V and Φ_o refer to the steady flow component, and

$$V = \nabla \Phi_o \tag{I-16}$$

so that $$\nabla \times V = 0 \tag{I-17}$$

The following expressions result from perturbing individual terms in Eq.(13), and dropping second order small quantities.

$$\partial^2\phi/\partial t^2 = -\omega^2\phi e^{i\omega t} \; ; \partial q^2/\partial t = 2i\omega V\cdot\nabla\phi e^{i\omega t}$$

$$q\cdot\nabla q^2 = V\cdot\nabla V^2 + 2(V\cdot\nabla)^2\phi e^{i\omega t} + [\nabla V^2]\cdot\nabla\phi e^{i\omega t}$$

$$\nabla^2\Phi = \nabla\cdot V + \nabla^2\phi e^{i\omega t}$$

Then these are substituted into Eq.(13), two equations result; a steady state equation

$$\frac{1}{2} V\cdot\nabla V^2 = c^2\,\nabla\cdot V \tag{I-18}$$

and a perturbation equation

$$\mathcal{L}\{\phi\} = 0 \tag{I-19}$$

where

$$\mathcal{L} = \nabla^2 + \frac{\omega^2}{c^2} - \frac{2i\omega}{c^2} V\cdot\nabla - \frac{1}{c^2}(V\cdot\nabla)^2 - \frac{1}{2c^2}[\nabla V^2]\cdot\nabla \tag{I-20}$$

The square bracket is intended to signify that the influence of the operator contained in it is restricted. Thus $[\nabla V^2]$ is a non-operating vector, while $(V\cdot\nabla)$ is a scalar operator.

Scheme for Obtaining Green's Equation

Equation (19) can be expressed in the more precise form

$$\mathcal{L}_r\{\phi(r)\} = 0 \tag{I-21}$$

where r is the vector coordinate of the "receiving" point. The subscript on the operator $\mathcal{L}$ indicates that its differential operator components, for example ∇_r, operate with respect to r. Next, a function G is assumed, satisfying the equation

$$\tilde{\mathcal{L}}_r\{G(\rho, r)\} = \delta(r-\rho) \tag{I-22}$$

The operator $\tilde{\mathcal{L}}$ is the adjoint of $\mathcal{L}$, and ρ is the vector coordinate of the "sending" or dummy point.

The following expression is now derived

$$G\mathcal{L}\{\phi\} = \phi\tilde{\mathcal{L}}\{G\} + \nabla\cdot P\{G;\phi\} \tag{I-23}$$

where $\mathbb{P}$ is the "bilinear concommitant". This is next integrated over the complete space $\mathcal{V}$ with dummy coordinate vector $\wp$ so that

$$\int_{\mathcal{V}} [G(\pi,\wp)\mathcal{L}_{\wp}\{\phi(\wp)\} - \phi(\wp)\tilde{\mathcal{L}}_{\wp}\{G(\pi,\wp)\}]\,d\mathcal{V} = \int_{\mathcal{V}} \nabla_{\wp}\cdot\mathbb{P}\{G(\pi,\wp);\phi(\wp)\}\,d\mathcal{V} \tag{I-24}$$

On substitution from Eqs.(21) and (22), and on using the divergence theorem

$$\phi(\pi) = -\int_{\mathcal{S}} \hat{\mu}\cdot\mathbb{P}\{G(\pi,\wp);\phi(\wp)\}\,d\mathcal{S} \tag{I-25}$$

where $\hat{\mu}$ is the unit outward normal on the surface $\mathcal{S}$ bounding the space $\mathcal{V}$.

The function G is variously referred to in the literature as the free-field Green's function, the unit solution, or when the operator is hyperbolic, the Reimann function. It will be referred to here simply as the Green's function, although this should more properly be reserved for the function which satisfies not only Eq.(22), but also the boundary conditions of the problem.

Derivation of Green's Equation

In order to express Eq.(23) in terms of the expression for $\mathcal{L}$ given in Eq.(20), the laws of product differentiation must be applied, term by term. First, these terms are considered separately, as follows

$$G\nabla^2\phi = \nabla\cdot G\nabla\phi - [\nabla G]\cdot\nabla\phi = \nabla\cdot G\nabla\phi - \nabla\cdot\phi\nabla G + \phi\nabla^2 G$$

$$G\frac{\mathbf{V}}{c^2}\cdot\nabla\phi = \nabla\cdot\frac{\mathbf{V}}{c^2}G\phi - \phi\,\nabla\cdot\frac{\mathbf{V}}{c^2}G$$

$$\frac{G}{c^2}(\mathbf{V}\cdot\nabla)^2\phi = G\frac{\mathbf{V}}{c^2}\cdot\nabla(\mathbf{V}\cdot\nabla\phi) = \nabla\cdot\frac{\mathbf{V}}{c^2}G(\mathbf{V}\cdot\nabla\phi) - [\mathbf{V}\cdot\nabla\phi]\nabla\cdot\frac{\mathbf{V}}{c^2}G$$

$$= \nabla\cdot\frac{\mathbf{V}}{c^2}G(\mathbf{V}\cdot\nabla\phi) - \nabla\cdot\mathbf{V}\phi(\nabla\cdot\frac{\mathbf{V}}{c^2}G) + \phi(\nabla\cdot\mathbf{V})^2\frac{G}{c^2}$$

$$\frac{G}{c^2}[\nabla V^2]\cdot\nabla\phi = \nabla\cdot[\nabla V^2]\frac{\phi G}{c^2} - \phi\,\nabla\cdot[\nabla V^2]\frac{G}{c^2}$$

Then using the above results, Eq.(23) becomes

$$G\{\nabla^2 + \frac{\omega^2}{c^2} - \frac{2i\omega}{c^2}\mathbf{V}\cdot\nabla - \frac{1}{c^2}(\mathbf{V}\cdot\nabla)^2 - \frac{1}{2c^2}[\nabla V^2]\cdot\nabla\}\phi$$

$$= \phi\{\nabla^2 + \frac{\omega^2}{c^2} + 2i\omega\nabla\cdot\frac{\mathbf{V}}{c^2} - (\nabla\cdot\mathbf{V})^2\frac{1}{c^2} + \nabla\cdot\frac{1}{2c^2}[\nabla V^2]\}G$$

$$+ \nabla\cdot\{G\nabla\phi - \phi\nabla G - \frac{2i\omega}{c^2}\mathbf{V}G\phi - \frac{\mathbf{V}}{c^2}G(\mathbf{V}\cdot\nabla\phi)$$

$$+ \mathbf{V}\phi(\nabla\cdot\frac{\mathbf{V}}{c^2})G - \frac{1}{2c^2}[\nabla V]^2 G\phi\} \qquad \text{(I-26)}$$

If the surface $\mathcal{S}$ bounds the flow, and is nonporous, then, on this surface

$$\hat{\mu} \cdot \mathbb{V} = 0 \tag{I-27}$$

and

$$\hat{\mu} \cdot \nabla_{\mathcal{P}} = \partial / \partial \mu \tag{I-28}$$

where μ is the local normal coordinate. Thus, identifying the bilinear concommitant in Eq.(26), and substituting into Eq.(25), using Eqs.(27) and (28)

$$\phi(\mathcal{R}) = \int_{\mathcal{S}} \left\{ \phi(\mathcal{P}) \frac{\partial G(\mathcal{R},\mathcal{P})}{\partial \mu} - G(\mathcal{R},\mathcal{P}) \frac{\partial \phi(\mathcal{P})}{\partial \mu} \right\} d\mathcal{S} \tag{I-29}$$

The Green's function $G(\mathcal{R},\mathcal{P})$ satisfies Eq.(22) in the $\mathcal{P}$ space, i.e.

$$\tilde{\mathcal{L}}_{\mathcal{P}} \{ G(\mathcal{R},\mathcal{P}) \} = \delta(\mathcal{R} - \mathcal{P}) \tag{I-30}$$

where from Eq.(26)

$$\tilde{\mathcal{L}} = \nabla^2 + \frac{\omega^2}{c^2} + 2i\omega \nabla \cdot \frac{\mathbb{V}}{c^2} - (\nabla \cdot \mathbb{V}) \frac{1}{c^2} + \nabla \cdot \frac{1}{2c^2} [\nabla V^2] \tag{I-31}$$

Normal Flow at a Boundary

Equation (29) gives the perturbation velocity potential at any point in the volume $\mathcal{V}$. Generally, the problem is to solve for the velocity potential at any point on the boundary given the normal flow velocities $\partial \phi / \partial n$,

where n is the local normal coordinate to the boundary at point r. Thus, from Eq.(29), an integral equation is obtained in ϕ as follows

$$\frac{\partial \phi(r)}{\partial n} + \int_S \frac{\partial \phi(p)}{\partial \mu} \frac{\partial G(r,p)}{\partial n} dS = \int_S \phi(p) \frac{\partial^2 G(r,p)}{\partial n \partial \mu} dS \qquad \text{(I-32)}$$

Assuming no radiation from infinity, the surface S consists of immersed bodies and any wake which sustains potential jumps.

Uniform Flow Over Thin Airfoil

A thin airfoil and its wake are shown in Figure 1. It is assumed to be a small angle of attack so that c and V are uniform everywhere, with V parallel to the x-axis, and of magnitude V.

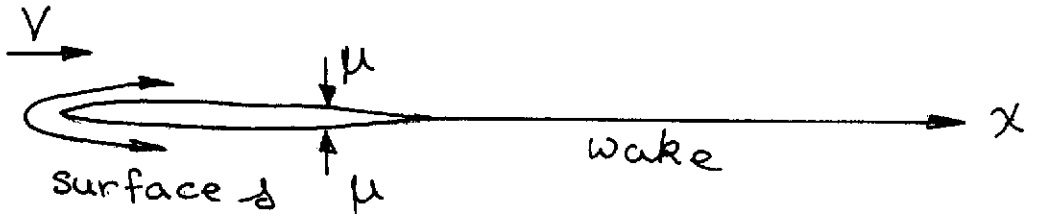

Figure 1. Thin Airfoil

It is clear that values of G on opposite sides of the airfoil are equal, while the local normals are equal and opposite. Thus the integrand containing $\partial\phi/\partial\mu$ cancels out, while, if the area of integration is transformed to a surface

S on one side of the airfoil and wake, as shown in Figure 2, ϕ in the second integrand is replaced by $\Delta\phi$, the velocity potential difference. If ν is the normal coordinate, as shown, then $\Delta\phi$ is positive when ϕ <u>decreases</u> in the positive ν direction.

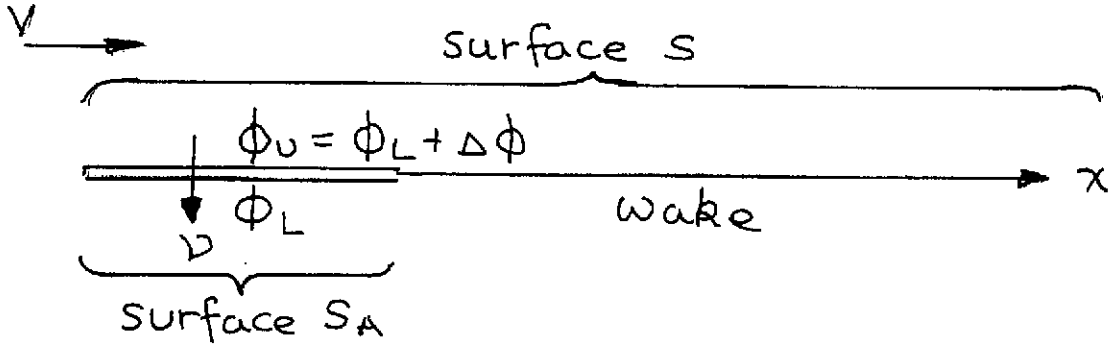

Figure 2. One-Sided Airfoil

Equation(32) now becomes

$$\frac{\partial\phi(\mathbf{r})}{\partial n} = \int_S \Delta\phi(\boldsymbol{\rho}) \frac{\partial^2 G(\mathbf{r},\boldsymbol{\rho})}{\partial n\, \partial \nu}\, dS \qquad \text{(I-33)}$$

The velocity potential perturbation can be related to the pressure potential perturbation by the equation

$$\phi(\mathbf{r}) = \frac{1}{V}\int_{-\infty}^{\mathbf{r}} \psi(\boldsymbol{\rho}')\exp\{i\omega(\lambda - x)/V\}\, d\lambda \qquad \text{(I-34)}$$

Therefore, Eq.(33) can be replaced by an integral equation in the pressure potential perturbation ψ, which can be written as

$$\frac{\partial\phi(\mathbf{r})}{\partial n} = \frac{1}{V}\int_{S_A} \Delta\psi(\boldsymbol{\rho}) \int_{\boldsymbol{\rho}}^{\infty} \frac{\partial^2 G(\mathbf{r},\boldsymbol{\rho}')}{\partial n\, \partial \nu} \exp\{i\omega(\boldsymbol{\rho} - \boldsymbol{\rho}')/V\}\, d\lambda\, dS \qquad \text{(I-35)}$$

where both paths of integration are parallel to the χ -axis, λ is the dummy variable for χ , and $\wp'$ is a point on this line whose χ -coordinate is λ . After rearranging the limits of integration, the area of integration S_A is restricted to the lifting surface only, as shown in Figure 2, because a pressure differential cannot be sustained by the wake. The net pressure Δp equals $-\rho_0 \Delta \psi$.

The Green's Function and the Source Solution in the Uniform Case

Under the conditions of uniform flow over a thin airfoil, the operators reduce to the form

$$\mathcal{L} = \nabla^2 - \left(\frac{i\omega}{c} - \frac{V}{c} \cdot \nabla \right)^2 \qquad \text{(I-36)}$$

$$\tilde{\mathcal{L}} = \nabla^2 - \left(\frac{i\omega}{c} + \frac{V}{c} \cdot \nabla \right)^2 \qquad \text{(I-37)}$$

clearly $\mathcal{L} = \tilde{\mathcal{L}}$ (I-38)

Therefore $\mathcal{L}$ is Hermetian, also $\mathcal{L}$ and $\tilde{\mathcal{L}}$ exchange roles when the flow direction reverses.

It can be shown that

$$G(\wp, \pi) = G^*(\pi, \wp) \qquad \text{(I-39)}$$

therefore,

$$\tilde{\mathcal{L}}_\pi \{G(\wp, \pi)\} = \mathcal{L}^*_\pi \{G^*(\pi, \wp)\} = \mathcal{L}_\pi \{G(\pi, \wp)\} \qquad \text{(I-40)}$$

and Eq.(22) can be reexpressed as

$$\mathcal{L}_{\Gamma}\{G(\Gamma,\rho)\} = \delta(\Gamma-\rho) \qquad \text{(I-41)}$$

giving, directly, the form of Green's function used in Eqs.(33) or (35).

However, it $S(\Gamma,\rho)$ represents a pulsating source located at the point ρ , it satisfies the equation

$$\mathcal{L}_{\Gamma}\{S(\Gamma,\rho)\} = \delta(\Gamma-\rho) \qquad \text{(I-42)}$$

thus S and G are identical. This fact has been assumed a-priori by most investigators, whereas, properly, it should have been derived from the Hermetian property of the operator $\mathcal{L}$ in the uniform flow case.

Conclusions

Following the approach taken in the uniform flow case, it might appear correct to obtain, or at least to approximate, a source type solution, and to use it in place of the Green's function. However, since this would satisfy the equation

$$\mathcal{L}_{\Gamma}\{S(\Gamma,\rho)\} = \delta(\Gamma-\rho) \qquad \text{(I-43)}$$

it can be seen, by comparison with Eq.(30) that S and G are different. Not only is the operator $\mathcal{L}$ given in Eq.(20) different in form to the operator $\tilde{\mathcal{L}}$ given in Eq.(31), but S as described by Eq.(43) represents a source centered at

the point $\wp$ whereas G as described by Eq.(30) represents a disturbance centered at the point $\wp$.

A physical explanation might be as follows. The cause of the potential perturbation is the normal flow or "downwash" perturbation on the surface. The result is the potential discontinuity. Therefore, it is incorrect to replace the potential discontinuity by a distribution of sources (in doublet form) because this reverses cause and effect.

In conclusion, a ray tracing method based on using the wave equation, and on tracing from the "potential perturbation" point towards the "downwash" point, is bound to lead to incorrect results in the non-uniform flow case. However, if the adjoint equation is used, with the ray originating at the "downwash" point, and terminating at the "potential perturbation" point, realistic results might be obtained. This reverses the normally accepted roles of "disturbing" and "receiving" points.

PART II

APPLICATION OF MONTE CARLO METHOD TO ACOUSTICAL ANALYSIS

II-1 DISCUSSION

Although analytical solutions to many acoustical problems have been known for many years, numerical techniques for the solution of acoustical problems involving arbitrary boundary conditions have lagged numerical developments in other fields, for example, finite element methods in structural analysis. In fact one method of acoustical analysis which has shown some promise has been the development of finite fluid element methods, such as those by Ziekiewicz and Chang[18] and Oden[19].

An attempt was made, under this grant, to develop a Monte Carlo method for the solution of acoustical field problems involving arbitrary distributions of sources and boundary conditions.

As a preliminary step, the proposed method was applied[3] to a relatively simple problem involving a single sound source in a rectangular room. A reasonable degree of success was achieved, but it was found that many computer hours would be required to obtain accurate results.

The method was then applied[4] to a problem involving a circular duct, for which an analytical solution was also available. Again, a reasonable degree of success was

achieved, but indications were that much more computer time would be needed for accurate results.

In evaluating such results, it must be borne in mind that the Monte Carlo method is capable of solving problems involving arbitrary boundaries, for which no other solutions are available. Therefore, the need for further development depends on the need for such solutions.

Two further lines of development remained unexplored at the termination of this work. These were

(a) Adaptation of the method to moving media, such as within the duct or nozzle of a jet engine.

(b) Adaptation of the method to problems involving diffractive scattering. This is a severe limitation, for example, although a rectangular room and a circular duct have been analyzed, a room with an open window, or an open ended duct, cannot be handled.

The two applications mentioned above are discussed in more detail in the following sections. Listings of computer programs are to be found in Reference 4.

II-2 CONTEMPORARY WORK IN THE FIELD

The first application of the Monte Carlo method to acoustics appears to have been by Allred and Newhouse[20, 21], who applied it to the determination of mean free paths of acoustical rays in rooms in order to estimate reverberation times. Their work contained an apparent procedural error pointed out by Hunt[22], and by Schroeder[23]. Schroeder and Kuttruff[24, 25], applied the Monte Carlo method to the determination of the rates of occurrence of maxima in the response of a room. In a later work, Schroeder[26] showed that the standard deviation of the fluctuation obtained by this method agrees closely with analytical predictions. In a paper on the digital simulation of reverberations in rooms, Schroeder[27] proposes the use of the Monte Carlo method for tracing rays, with the suggestion that the amplitude of these rays be attenuated after successive collisions with the walls. Whereas, in the above references, the Monte Carlo method was employed to obtain statistical information on mean free paths of rays, and to estimate the occurrence of maxima, the present Monte Carlo application[28] is directly aimed at obtaining solutions to acoustical field problems. Thus the end result is a time history of the pressure at a given point in the field.

II-3 APPLICATION TO RECTANGULAR ROOM PROBLEMS

Introduction

In attempting to set up a Monte Carlo method for acoustics, the author, with Thanedar, selected the direct representation of the acoustical pressure as the quantity to be determined. This does satisfy the wave equation, but is not a quantity which satisfies conservation laws. Therefore, for example, the pressure in a region is not directly proportional to the number of rays passing through it. However, an algorithm has been developed for local pressure which does depend on the characteristics of the rays passing through a small region, which is referred to as a "test cell".

The process of ray tracing used in the Monte Carlo method starts with selection of a ray tube pulse of appropriate weight, originating at a source. Each ray, in turn, is traced through all of its interactions with the boundaries, which may result in reflection, or, if the boundaries are assumed to be absorbent, in the chance of a sudden death. Tracing of a particular ray is terminated when the required solution time has elapsed if it has not already suffered sudden death. During all of this time, the pressure-time history is accumulated at 'receiving' points by using the appropriate algorithm.

Definitions

C = Velocity of sound

$D\{\}$ = Variance of a quantity

$E\{\}$ = Expected value of a quantity

i = Index on source pulse

I = Upper limit on i

j = Index on time step

J = Upper limit on j

k = Index on sample

K = Upper limit on k

M = Mass of air

n = Index for ray count

N = Upper limit on n

N_p = Total number of pulses

P = Total atmospheric pressure

P_o = Static pressure

Q = Source strength

R = Distance travelled by ray

S = Index

t = Time

T_p = Time duration of a pulse

V = Volume

W = Statistical weight

$\Delta\chi$ = Increment of a quantity χ

ρ = Density

τ = Time related to a pulse

σ = Standard deviation

Ω = Solid angle

Calculation of Acoustical Pressures

The rectangular room enclosure, with a single monopole source, is shown in Figure 3. A typical source time history $Q(t)$ of duration T_p is shown in Figure 4, this is approximated by square pulses of width Δt, and of strength Q_i, $i = 1$ to I, originating at time $T_i (= [i - 1/2]\Delta\tau)$. It may be noted that Q has the dimensions of rate of change of volume flow rate, so that the volume flow rate will only return to zero if the integral of Q returns to zero, i.e., if

$$\sum_{i=1}^{I} Q_i \Delta\tau = \int_0^{T_p} Q(t)\,dt = 0 \qquad \text{(II-1)}$$

where $I = T_p/\Delta\tau$. Otherwise the mean pressure in an enclosure will steadily rise as air is injected into it.

In the absence of boundaries, the acoustical pressure increment $\Delta p(t)$ at a receiving point is given by

$$\Delta p(t) = p(t) - P_o = \rho Q(t - R/c)/4\pi R \qquad \text{(II-2)}$$

where R is the distance from the source to the point, $p(t)$ is the total pressure, P_o the ambient pressure, c the velocity of sound and ρ ambient air density. When the boundaries form a rectangle, the effects of multiple reflections can be handled with relative simplicity. If the infiinte set R_s, $S = 1$ to ∞, represents all

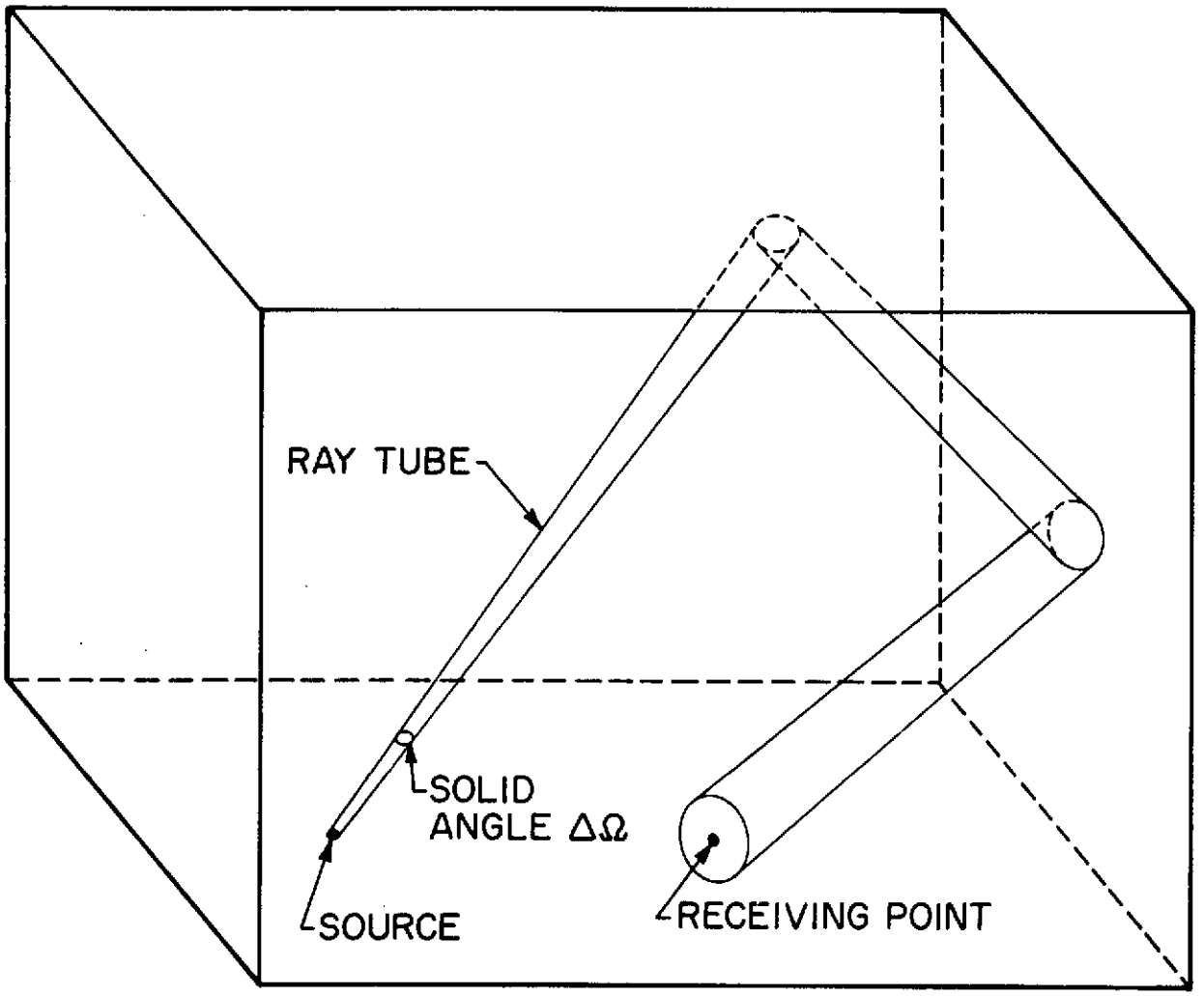

Fig. 3 Rectangular Room Problem

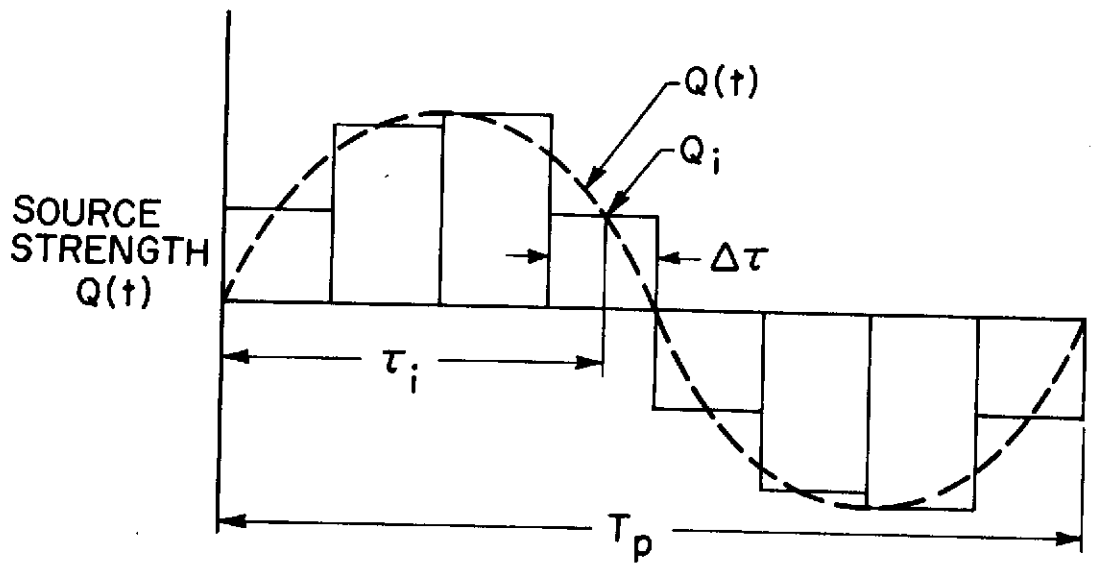

Fig. 4 Typical Source Strength Time History

of the possible distances travelled by an acoustical ray from the source to the point in question, then the pressure at that point is

$$\Delta p(t) = \sum_{s=1}^{\infty} \rho Q(t - R_s/c)/4\pi R_s \qquad \text{(II-3)}$$

This result can be visualized more clearly by the method of images. If each wall, and each image of a wall, is replaced by its image, an infinite array of image rooms can be constructed, each containing a source, as shown in Figure 5. Then the pressure at the receiving point is the sum of the effects of all of these image sources, as well as the true source.

Consider, now, the influence of some randomly selected ray pulse, let this be the n^{th} pulse selected, and let the pulse have a strength Q_n and initial time τ_n which has been selected at random out of the values τ_i, $i = 1$ to I. Further, let its influence be confined to a ray tube of solid angle $\Delta\Omega$, with randomly selected direction cosines, using, for example, the method of selection given by the author[29].

(This method selects sets of direction cosines at random out of a population having a uniform probability density distribution with respect to solid angle. Thus spherical symmetry is preserved).

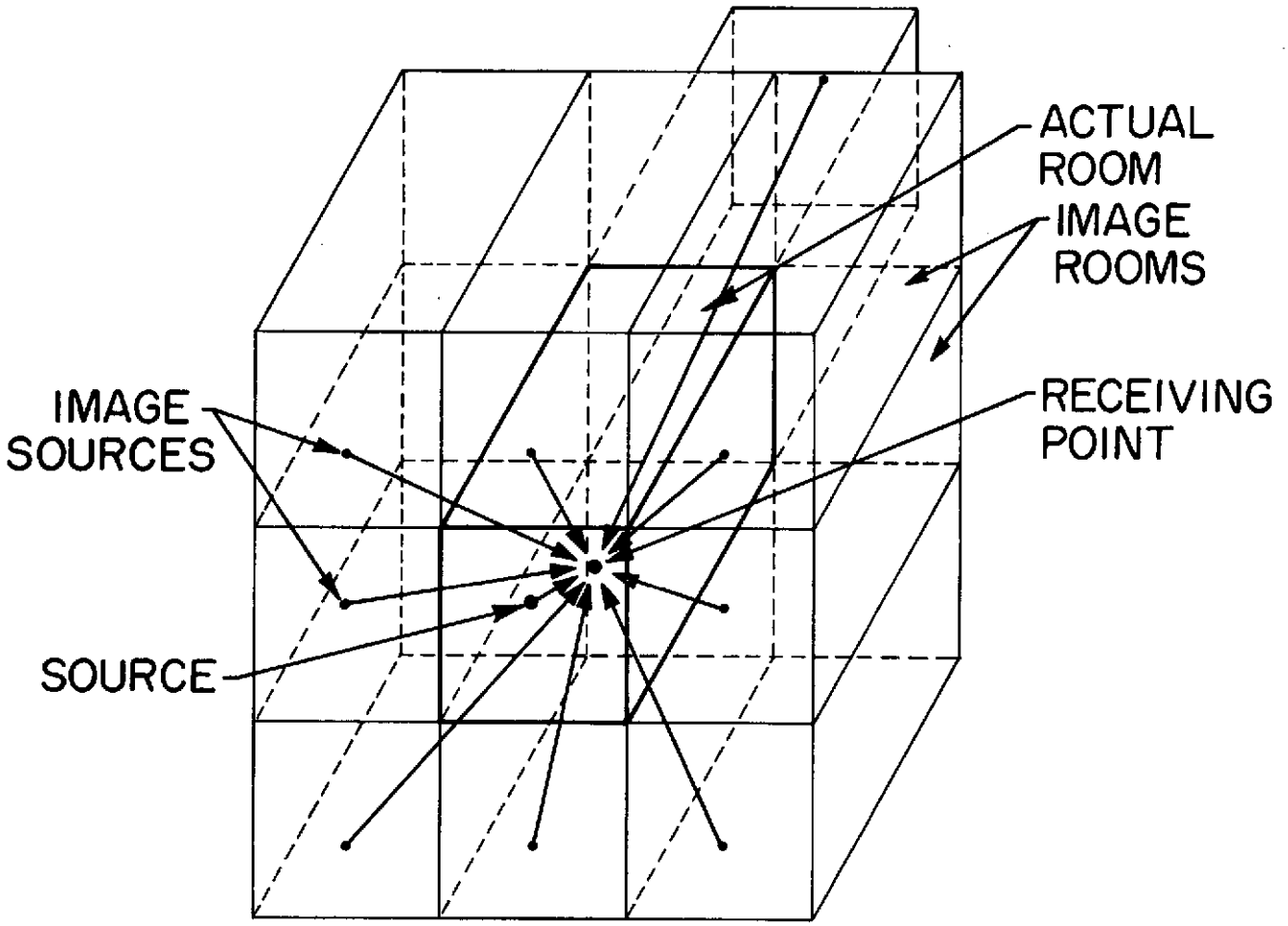

Fig. 5 Array of Image Rooms

Then, if the receiving point is contained within the ray tube for the s^{th} time at a distance R_{ns} from the source, measured through all of the reflections, the effect on the pressure increment at the receiving point is represented by a δ - function, resulting in

$$\Delta p_{ns}(t) = \rho \Delta T Q_n \delta(t-\tau_n-R_{ns}/c)/4\pi R_{ns} \quad \text{(II-4)}$$

If time t is divided up into J time cells of duration Δt, and if Δp_{nj} is the mean value of $\Delta p_{ns}(t)$ taken over the j^{th} time interval, then, from Eq. 4

$$\Delta p_{nj} = (1/\Delta t) \int_{(j-1)\Delta t}^{j\Delta t} \Delta p_{ns}(t)\, dt$$

$$= \rho \Delta T Q_n / 4\pi \Delta t R_{ns} \quad \text{if the ray passes for the } s^{th} \text{ time during the } j^{th} \text{ interval}$$

$$= 0 \quad \text{otherwise} \qquad \text{(II-5)}$$

Although the method just described is under consideration for the case of curved boundaries, a simpler alternate method is possible for rectangular boundaries, in which a small fixed test cell of volume ΔV is set up, and ΔR_{nj} is determined, the distance by which the n^{th} ray penetrates the volume ΔV in the j^{th} time interval. At the same time, the value of $\bar{R}_{nj}$, the mean distance from the source during penetration, is obtained. Then $R_{ns} \approx \bar{R}_{nj}$. The two methods are shown in Figure 6. Clearly, ΔR must be normalized by dividing by a characteristic length which

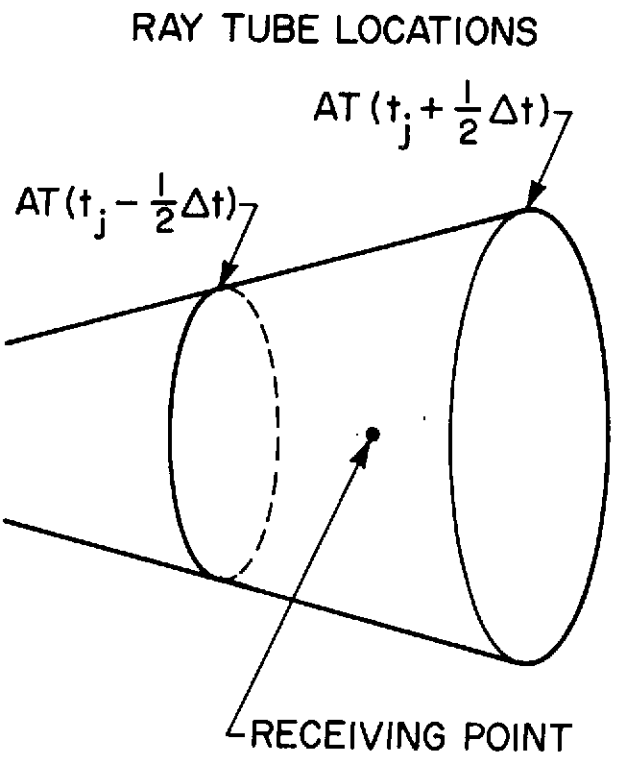

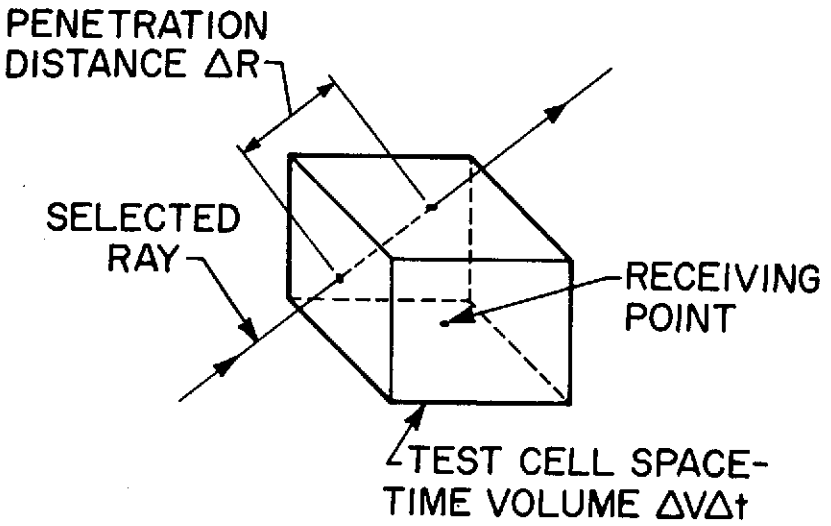

Fig. 6 Alternate Methods of Accumulating Acoustical Pressure Contributions

includes the ratio of relative cross section areas of the volume ΔV and of the ray tube, i.e., by

$$\Delta R_{norm} = \Delta V / \bar{R}_{nj}^2 \Delta\Omega \qquad \text{(II-6)}$$

so that the pressure increment given by Eq. 5 is now written as

$$\Delta p_{nj} \approx \rho \Delta\tau \Delta\Omega Q_n \bar{R}_{nj} \Delta R_{nj} / 4\pi \Delta t \Delta V \qquad \text{(II-7)}$$

Finally, the expected pressure is obtained by averaging over all of the N pulses followed, where $n = 1$ to N, and by normalizing by multiplying by the total number of pulses N_p which could have been selected, i.e., by

$$N_p = 4\pi I / \Delta\Omega = 4\pi T_p / \Delta\Omega \Delta\tau \qquad \text{(II-8)}$$

Thus the algorithm for the pressure increment in the j^{th} time interval is obtained by averaging the pressure disturbances and then substituting from Eqs. 7 and 8, which leads to

$$\Delta p_j = (N_p/N) \sum_{n=1}^{N} \Delta p_{nj}$$

$$= (\rho T_p / N \Delta V \Delta\tau) \sum_{n=1}^{N} Q_n \bar{R}_{nj} \Delta R_{nj} \qquad \text{(II-9)}$$

It may sometimes be desirable to present this algorithm in the dimensionless form

$$\Delta p_j / \rho c^2 = (T_p / N c^2 \Delta V \Delta T) \sum_{n=1}^{N} Q_n \bar{R}_{nj} \Delta R_{nj} \qquad \text{(II-10)}$$

Calculation of Standard Deviations

Since the results of a Monte Carlo calculation are statistical samples, it is important that we know their standard deviation. In order to do this, the calculation implied in Eq. 9 is made in K blocks, each consisting of N_k selected ray pulses. Each selection is given equal statistical weight, so that the statistical weight of the k^{th} batch is:

$$W_k = N_k / N \qquad \text{(II-11)}$$

Now we modify Eq.9 slightly, and write

$$(\Delta p_j)_k = (\rho T_p / N_k \Delta V \Delta T) \sum_{n=1}^{N_k} Q_n \bar{R}_{nj} \Delta R_{nj} \qquad \text{(II-12)}$$

It is clear that

$$\Delta p_j = \sum_{k=1}^{K} W_k (\Delta p_j)_k \qquad \text{(II-13)}$$

Then the variance of the acoustical pressure is

$$D^2\{\Delta p_j\} = \sum_{k=1}^{N} W_k^2 \{(\Delta p_j)_k - \Delta p_j\}^2 = \sigma_{\Delta p}^2 \qquad \text{(II-14)}$$

where $\sigma_{\Delta p}$ is the standard deviation of the predicted acoustical pressure.

A flow diagram showing the computer logic necessary to perform these calculations is given in Figure 7.

Verification of Method Applied to Rectangular Room

It is prudent to check the consistency of a method such as this by considering the results which would be obtained by solving very simple problems. The first solution considered was that of a source in an unbounded medium. The second was that of the ultimate average pressure to be expected in a rectangular room. Both are treated in the following sections by evaluating the algorithm given in Eq.9 and then comparing with the known solutions.

Source in Unbounded Medium

The problem is illustrated in Figure 8. A source which has a constant strength Q over a total period T_p $(>>\Delta t)$ is surrounded by an annular test volume of mean radius R and thickness ΔR. Clearly, every selected ray penetrates this volume for a distance $\Delta R_{nj} = \Delta R$ at a mean distance of $\bar{R}_{nj} = R$. The number of rays penetrating the control volume during the period Δt is $N\Delta t / T_p$, and the test cell volume ΔV is $4\pi R^2 \Delta R$. Substituting these values into Eq.9, the pressure increment becomes

$$\Delta p_j = \rho Q / 4\pi R \qquad \text{(II-15)}$$

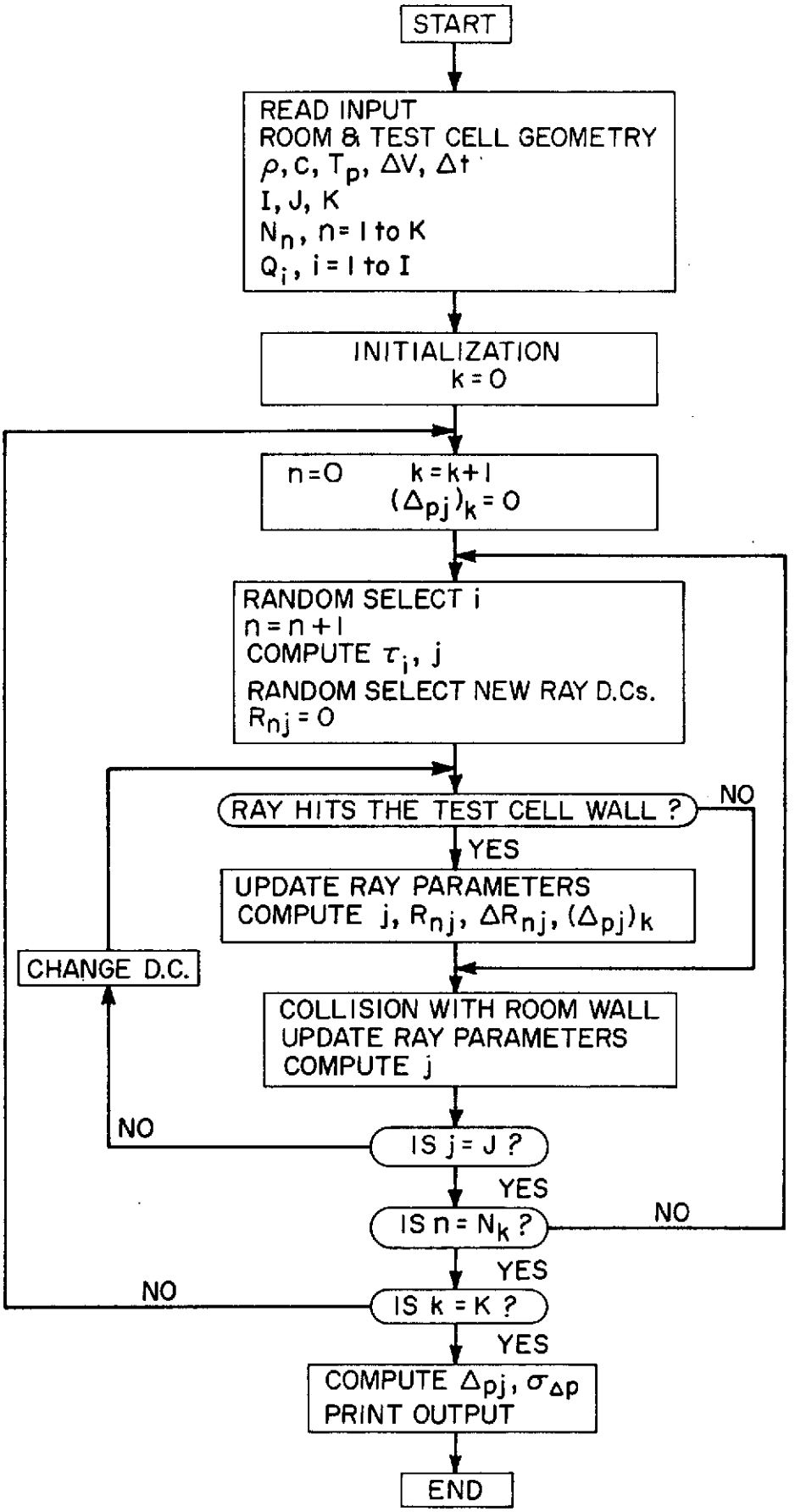

Fig. 7 Flow Diagram of Monte Carlo Method Applied to Rectangular Room Problem

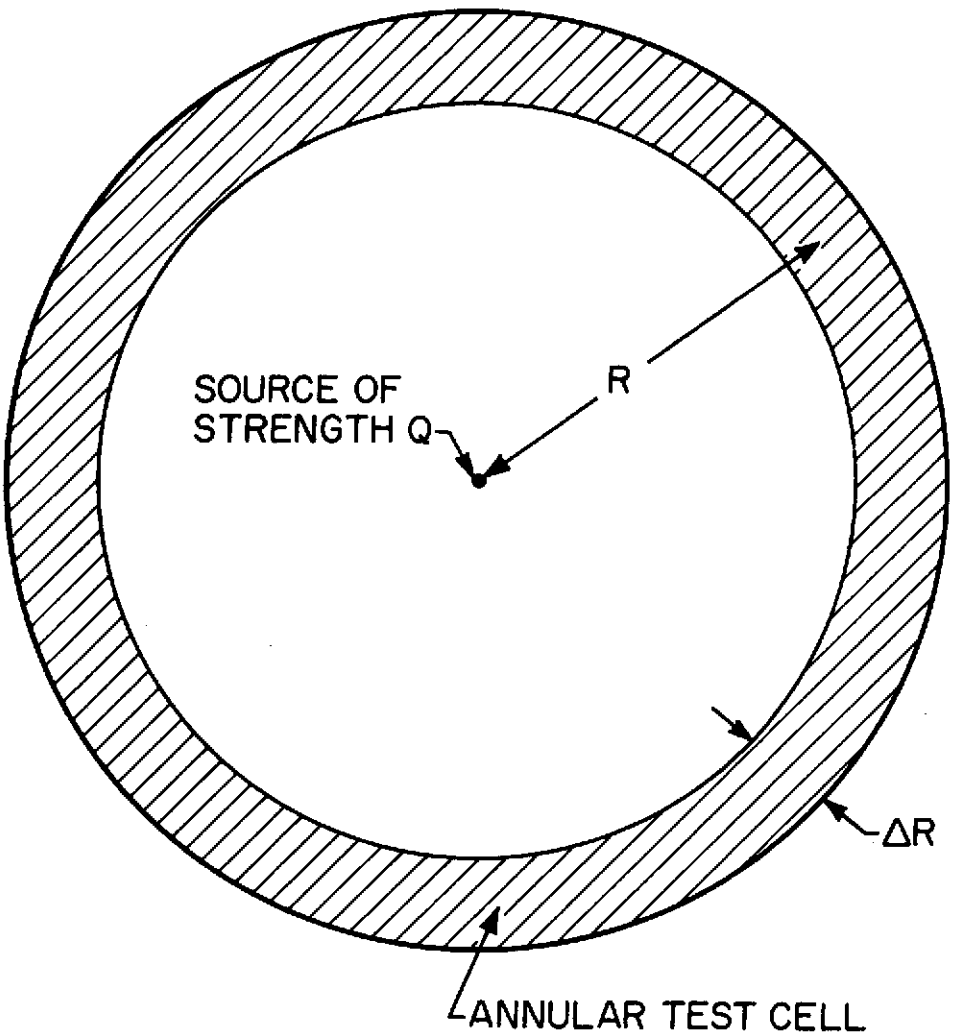

Fig. 8 Source in Unbounded Medium

which is the known analytical solution for the problem.

Source in Bounded Medium

The total air mass introduced into the room by the source is equal to

$$\Delta M(t) = \rho \int_0^t \int_0^\tau Q(\mu) d\mu d\tau$$

$$= \rho [\tau \int_0^\tau Q(\mu) d\mu]_0^t - \rho \int_0^t \tau Q(\tau) d\tau \qquad \text{(II-16)}$$

If the source strength $Q(t)$ meets the condition given by Eq.1 that it should cut off at time T_p , i.e.,

$$\int_0^t Q(\mu) d\mu = 0 ; \quad t > T_p \qquad \text{(II-17)}$$

then, for all times $t > T_p$, the final mass introduced into the room becomes

$$\Delta M = -\rho \int_0^{T_p} \tau Q(\tau) d\tau \qquad \text{(II-18)}$$

and, provided that this is small compared to the mass ρV already in the room, where V is its volume, the expected value of the adiabatic pressure rise in the room, $E\{\Delta p(t)\}$ is equal to

$$E\{\Delta p(t)\} = c^2 \Delta M / V$$

$$= -(\rho c^2 / V) \int_0^{T_p} \tau Q(\tau) d\tau ; \quad t > T_p \qquad \text{(II-19)}$$

If Q is described in terms of equivalent pulses, as in Figure 4, then for $t_j > T_p$

$$E\{\Delta p(t_j)\} = -(\rho c^2 \Delta T/V)\sum_{i=1}^{I} T_i Q_i \qquad \text{(II-20)}$$

Now consider the expected adiabatic rise predicted by the Monte Carlo method, using Eq.9. Because selection of any one of the I pulses is equally possible, it is readily shown that

$$E\{\Delta p_j\} = (\rho T_p / N \Delta V \Delta t) E\left\{\sum_{n=1}^{N} Q_n \bar{R}_{nj} \Delta R_{nj}\right\}$$

$$= (\rho c \Delta T/\Delta V \Delta t)\, E\{\Delta R\} \sum_{i=1}^{I} (t_j - T_i) Q_i \qquad \text{(II-21)}$$

The expected value of the penetration distance $E\{\Delta R\}$ is best obtained by using the method of images as shown in Figure 9, and by considering the effect of all of the image sources. The total number of such images which can influence Δp_j is the number in an annular spherical volume of radius $c(t_j - T_i)$ and thickness $c\Delta t$. Since there is one source per room of volume V, the total number is

$$4\pi c^3 (t_j - T_i)^2 \Delta t / V$$

This number is actually equal to the number of reflections in the room during the corresponding period.

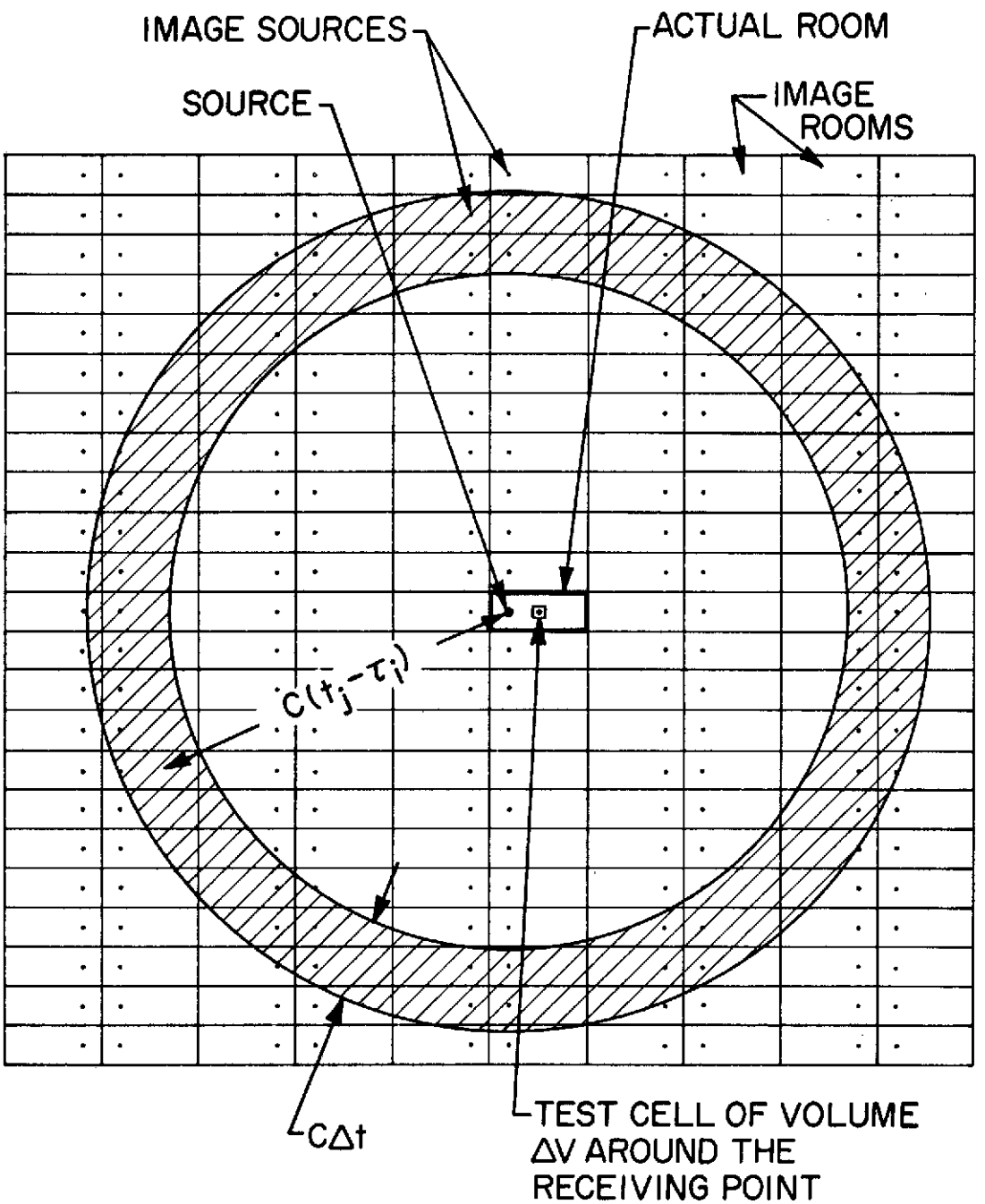

Fig. 9 Average Pressure by Image Method

The expected penetration into the test cell ΔV of any ray from one of these image sources

$$\left(\Delta V / 4\pi c^3 (t_j - \tau_i)^2 \Delta t\right) \times (c \Delta t)$$

Therefore, the expected value of the penetration per pulse is the product of the above with the number of reflections.

$$E\{\Delta R\} = c \Delta V \Delta t / V \qquad \text{(II-22)}$$

Substituting into Eq.21, and assuming the cutoff condition given in Eq.1

$$E\{\Delta p_j\} = (\rho c^2 \Delta T / V) \sum_{i=1}^{I} (t_j - \tau_i) Q_i$$

$$= -(\rho c^2 \Delta T / V) \sum_{i=1}^{I} \tau_i Q_i \qquad \text{(II-23)}$$

which is in agreement with Eq.20 obtained by considering adiabatic compression.

Calculations for Rectangular Rooms

Double Rectangular Pulse

Two sets of calculations are presented here. The first assumed a double rectangular pulse of 0.2 seconds duration as shown in Figure 10. A drawing of the rectangular room, specifying the essential dimensions is shown in Figure 11. The supporting medium was considered to be air with a mass density ρ equal to 0.002378 slugs/ft^3 and a velocity of sound c equal to 1100 ft/sec. Taking the space-time volume (i.e. $\Delta V \Delta t$) of the test cell to be

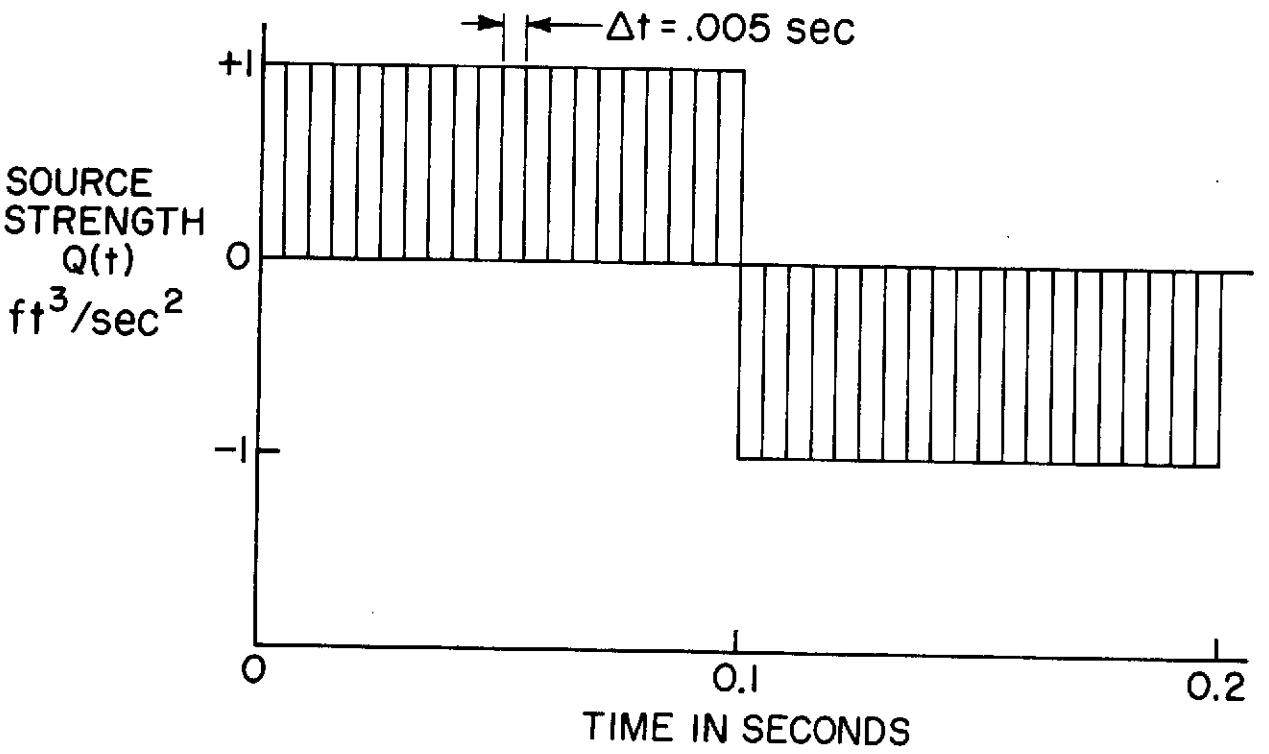

Fig. 10 Rectangular Pulse

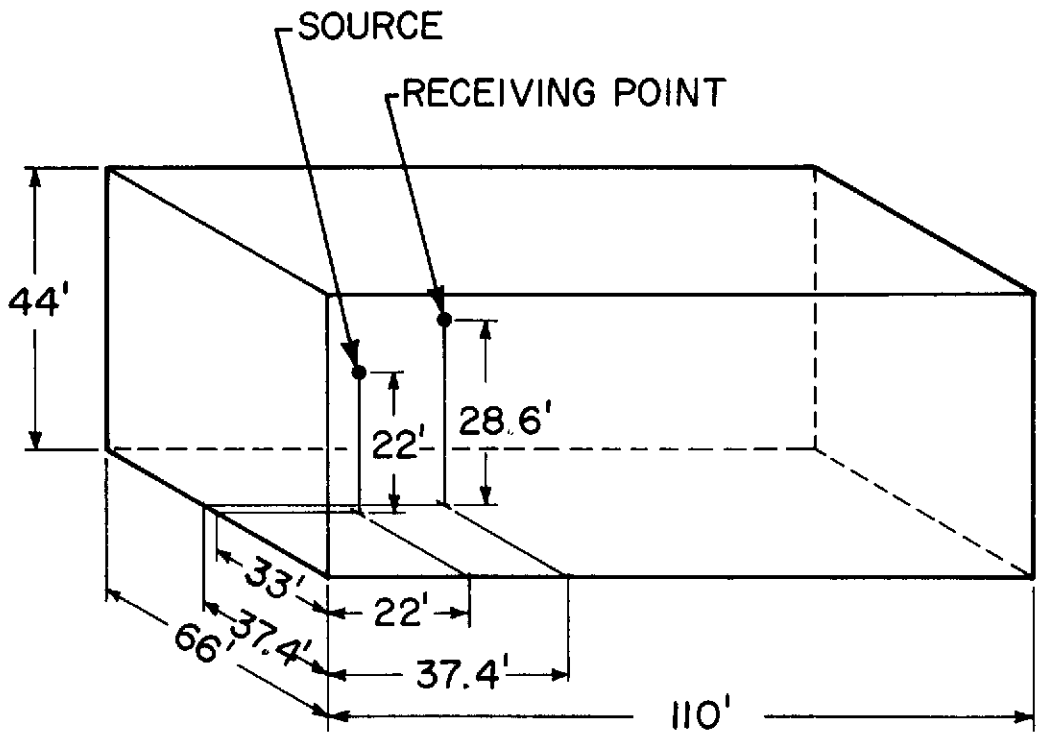

Fig. 11 Rectangular Room Used in Analyses

0.4259 ft^3-sec, five blocks of data were obtained including a total of 35000 selected ray pulses. These calculations are presented for the duration of the pulse in Figure 12, where results from the five blocks are shown separately, and the overall mean values are shown plus and minus one standard deviation. One would expect the correct result to be within these limits about 70% of the time. For comparison, the results obtained by Mintzer[30] using the Laplace transform approach are given in Figure 13.

One block of calculations for 5000 ray pulses was continued out to 0.4 seconds, twice the pulse duration. These results are shown in Figure 14, where they are compared with the expected adiabatic pressure rise as predicted by Eq.23.

One Cycle Sinusoidal Pulse

The second set of calculations was prepared for a comparison with calculations by the normal mode method. In order to make the results more convergent, a sinusoidal pulse was assumed, as shown in Figure 15. The Monte Carlo results are shown compared with the normal mode calculations in Figure 16. These calculations consisted of ten blocks totalling 50000 selected ray pulses, and took 211 seconds of core time on the CDC 6400 computer at the University of Virginia's Computation Center. The normal mode solution included all modes from (1,0,0) up to (15,15,15) and required 118 seconds. Therefore, computation times were comparable.

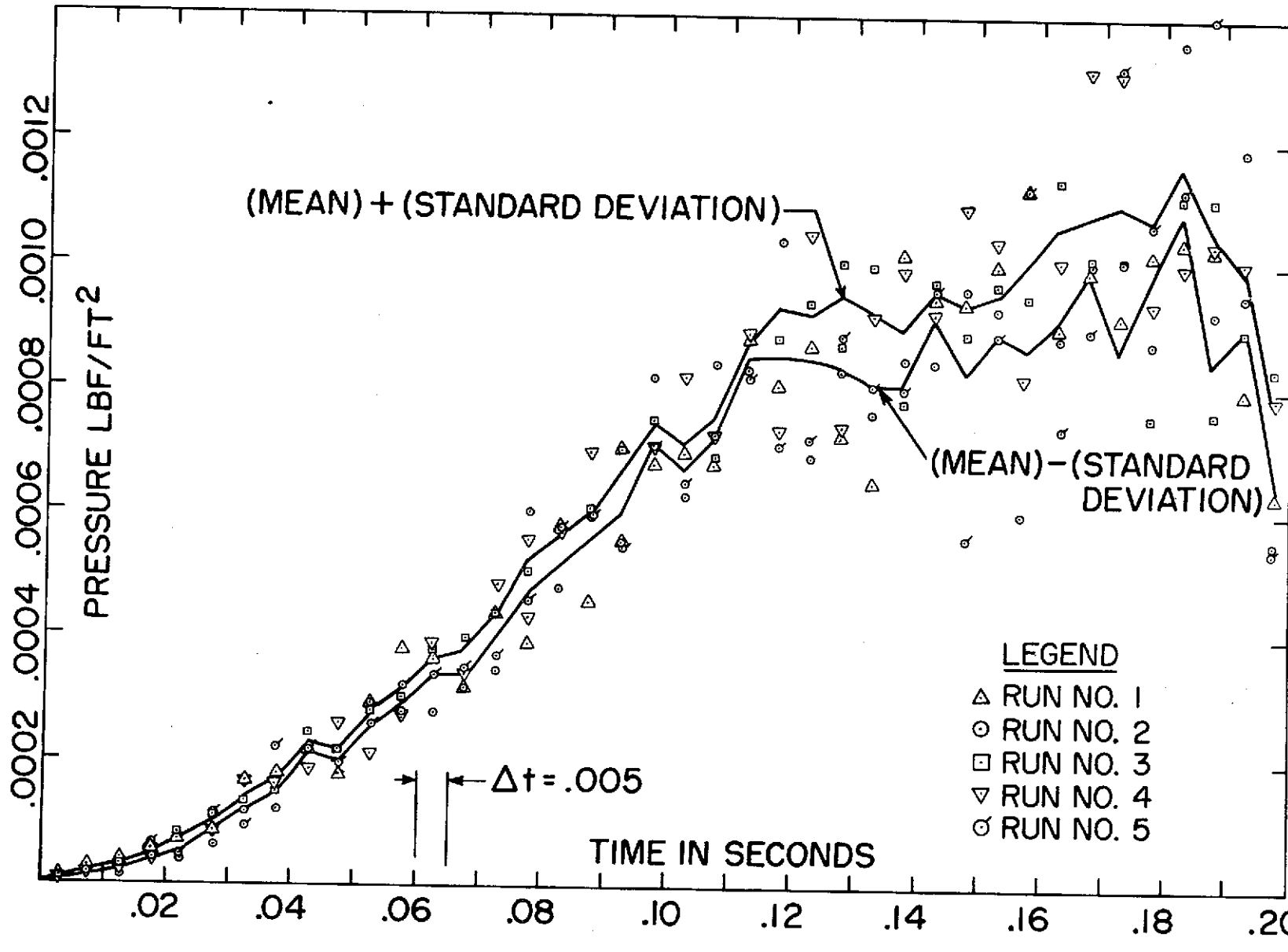

Fig. 12 Pressure Time History for Square Pulse in Rectangular Room

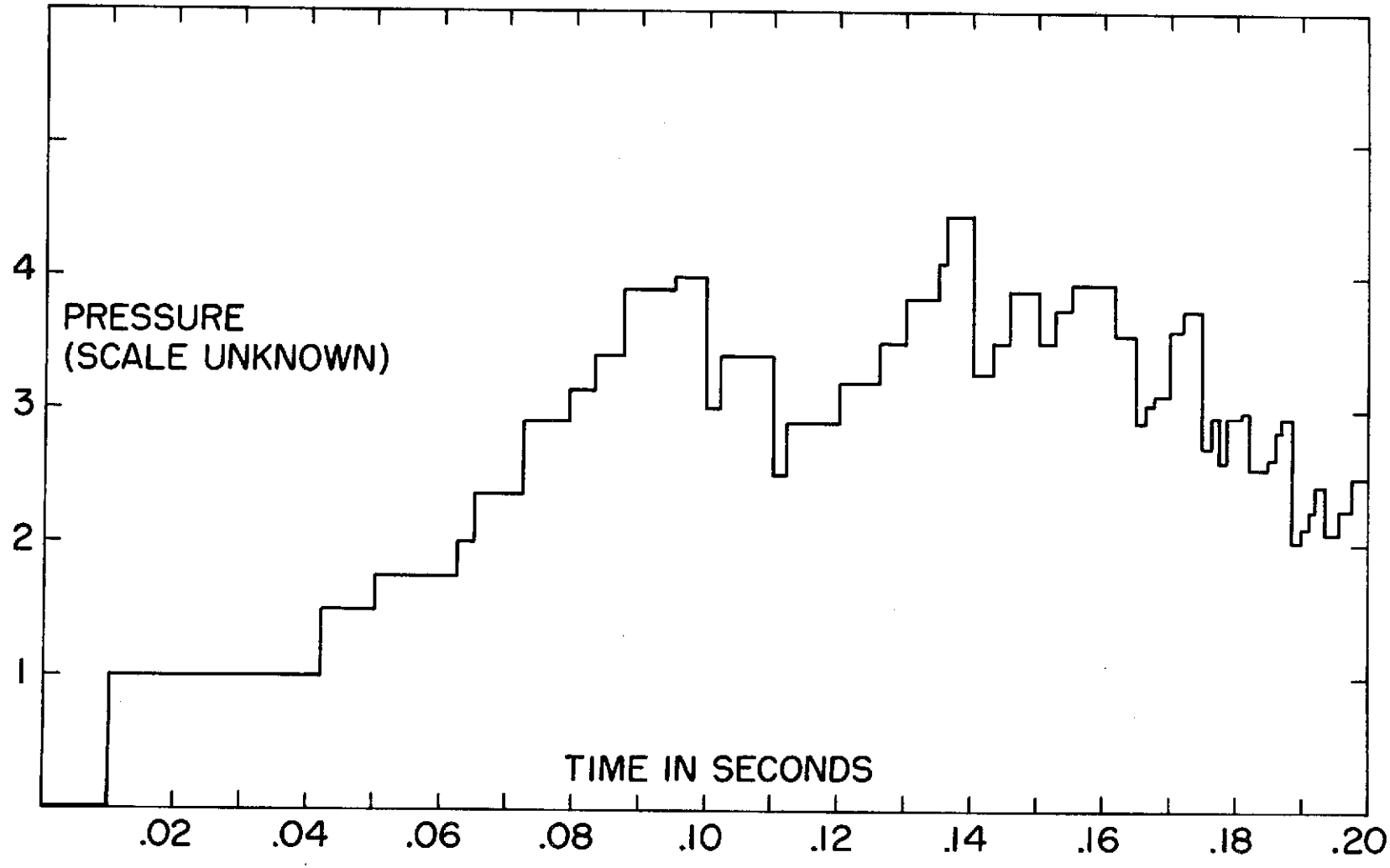

Fig. 13 Time History for Square Pulse in Rectangular Room - Mintzer's (1950) Results

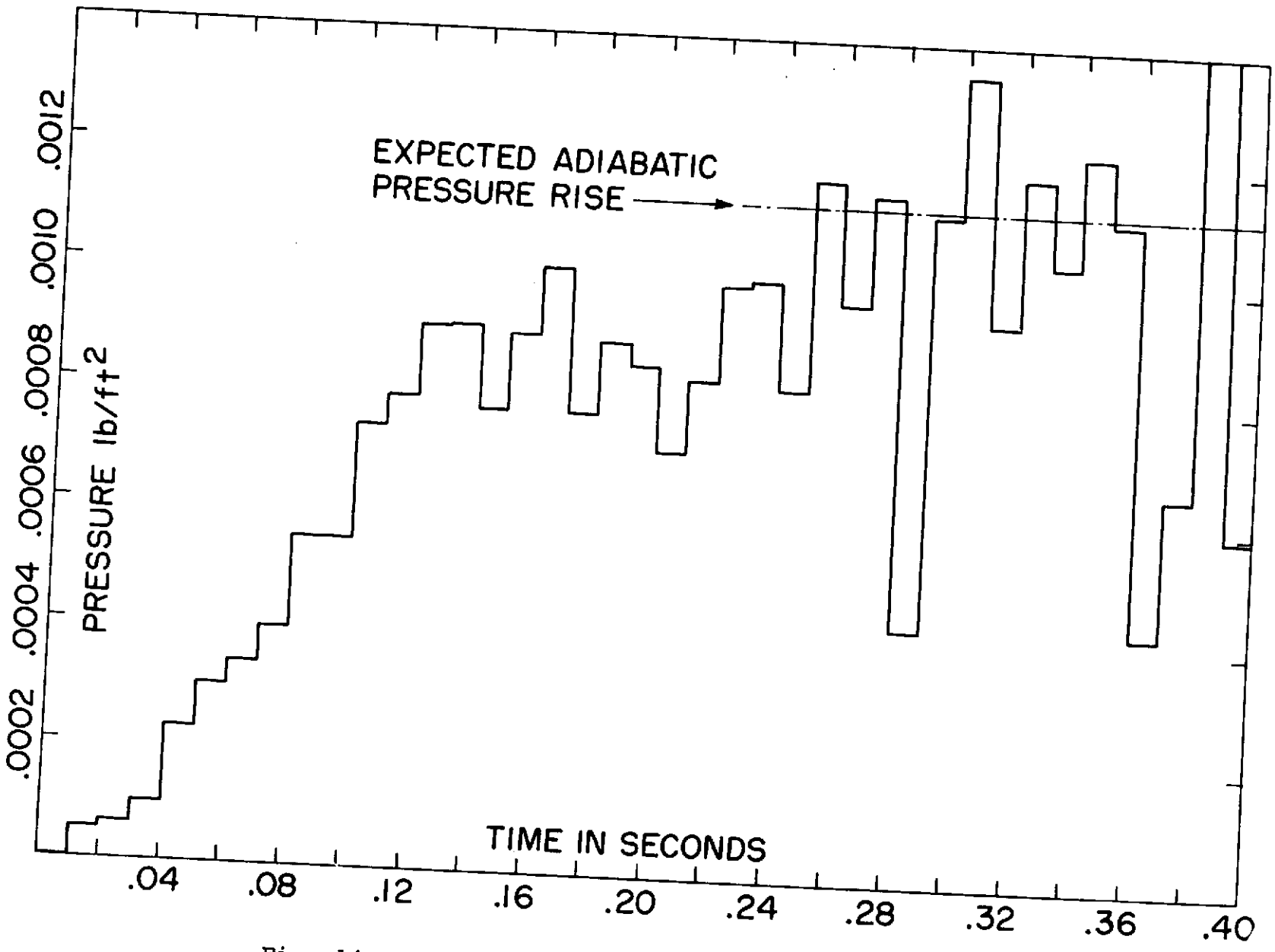

Fig. 14 Pressure for Extended Time - Square Pulse

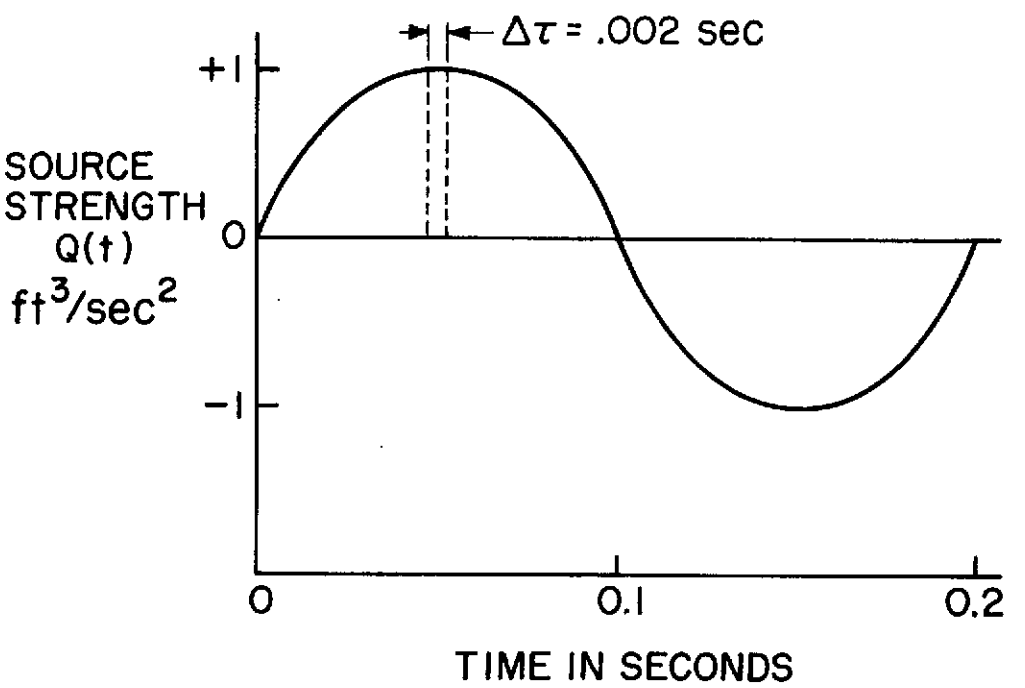

Fig. 15 Sinusoidal Pulse

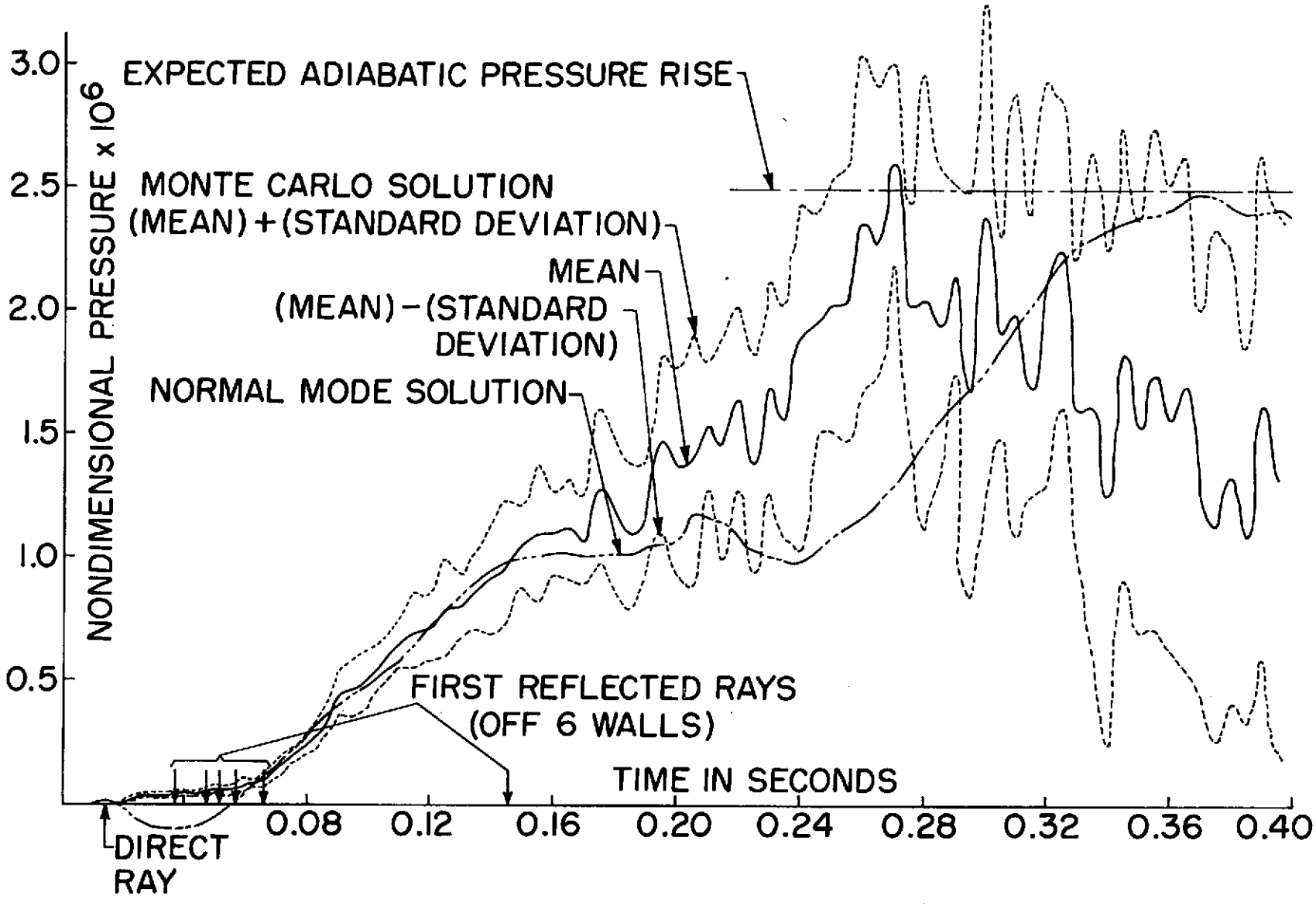

Fig. 16 Pressure Time History for Single Sinusoidal Pulse in a Rectangular Room

It will be seen that the results of the two methods are in general agreement, when it is considered that the normal mode solution should only be expected to be within the limits of plus or minus one standard deviation about 70% of the time.

II-4 APPLICATION TO CIRCULAR DUCT PROBLEMS

A solution[4] to the problem of a source at the closed end of a circular duct was obtained by a method which might be described essentially as follows.

A central ray was selected as in the rectangular room problem, and was traced through collisions with the cylindrical walls of the duct. In addition, two rays were selected making small angles with the central ray, so that the intersection of the three rays with a normal plane formed the vertices of a right angled triangle. These additional rays were traced.

The test volumes were small spheres, to simplify the calculation of the penetration distance ΔR. Whenever a test volume was penetrated, the intersections of the rays with a normal plane were found, and the area of the triangle so formed was calculated. The distance which would have been travelled by the originating bundle of rays to form the same area was calculated, and taken as R_{EQ}. The value so calculated was substituted in place of $\overline{R}_{nj}$ in Eq.(II-9)

A typical reflection of the three rays from a curved surface is illustrated in Figure 17, while a comparison of a Monte Carlo solution with a normal mode solution is shown in Figure 18. In both cases, a source on the center of the closed end of a 7.5" radius duct was assumed to emit for one cycle at a period of .002 seconds. The pressure was obtained at a point 10" from the end, and 3.16" from the axis.

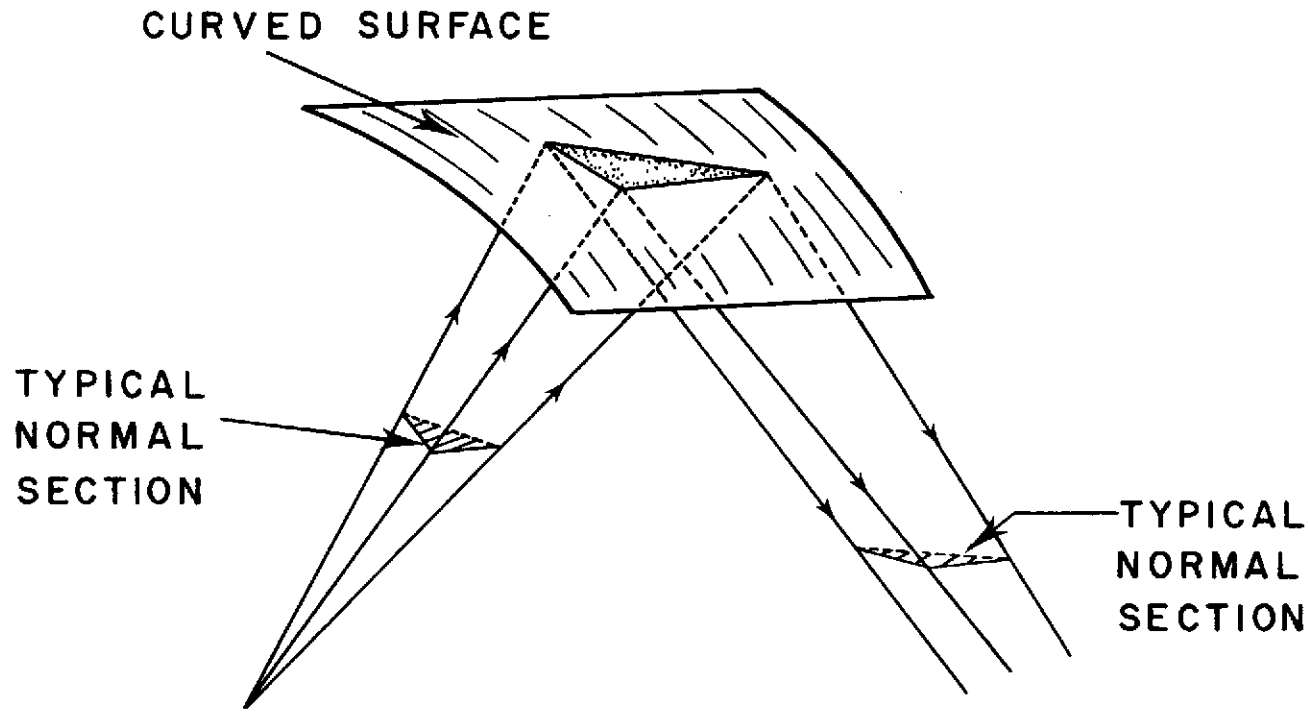

Fig. 17 Incident and Reflected Rays

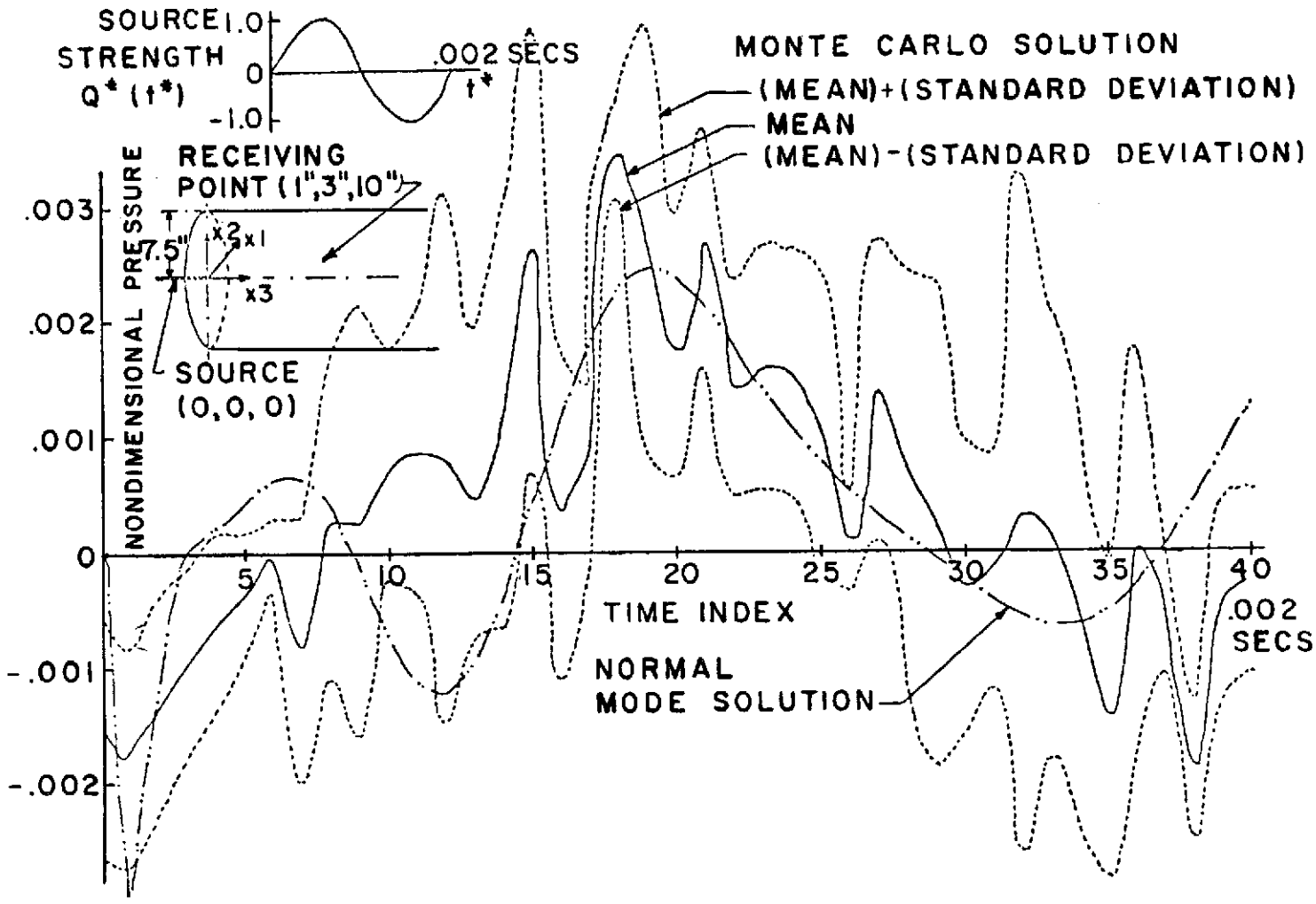

Fig. 18 Pressure vs Time for a Single Cycle Source at end of a Cylindrical Duct (Comparison of the Monte Carlo and the Normal Mode Solutions)

In these calculations, a total of 2500 ray pulses were followed, divided into five equal blocks for the purpose of estimating deviations. These took 189 seconds of core time on the CDC 6400, or .076 seconds per pulse. In contrast, the rectangular room solution required 211 seconds for 50000 ray pulses, or .0042 seconds per pulse. The nearly 20:1 time increase was due to the much greater complexity of handling the wall reflections, as well as the to the fact that three rays had to be traced in place of one.

REFERENCES

1. Haviland, J.K., "The Integral Equation for Small Perturbations of Irrotational Flows", AIAA Journal, to be published.

2. Haviland, J. K., and Yoo, Y. S., "Downwash-Velocity Potential Method for Oscillating Surfaces", AIAA Journal, 11, pp 607-612, 1973.

3. Haviland, J.K., and Thanedar, B.D., "Monte Carlo Applications to Acoustical Field Solutions", J. Acoustical Soc. of Am., to be published.

4. Thanedar, B. D., "Monte Carlo Investigation of Transient Acoustic Fields in Partially or Completely Bounded Media", Doctoral Dissertation, University of Virginia, October, 1972.

5. Andrew, L.V., and Stenton, T.E., "Unsteady Aerodynamics for Advanced Configurations, Part VII - Velocity Potentials in Non-Uniform Flow over a Thin Wing", Air Force Flight Dynamics Laboratory Report FDL-TDR-64-152, Part IV, 1968.

6. Landahl, unpublished, referred to by Andrew and Stenton in Ref. 5.

7. Bland, S.R., "Comments on NASA Langley Research on Transonic Unsteady Aerodynamics", NASA Langley Research Center, presented at 36th AGARD Structures and Materials Panel Meeting, Milan, Italy, 1973.

8. Landahl, M.T., "Linearized Theory for Unsteady Transonic Flow", Symposium Transonicum, K.Oswatitsch, ed., Springer-Verlag, Berlin, 1964, pp 414-439.

9. Ehlers, F.E., "A Finite Difference Method for the Solution of the Transonic Flow Around Harmonically Oscillating Wings," NASA CR-2257, 1973.

10. Stahara, S.S., and Spreiter, J.R. "Development of a Nonlinear Unsteady Transonic Flow Theory", NASA CR-2258, 1973.

11. Revell, "Research on Unsteady Transonic Flow Theory", NASA CR-112114, 1973.

12. Cunningham, A.M., "The Application of General Aerodynamic Lifting Surface Elements to Problems in Unsteady Transonic Flows", NASA CR-112264, 1973.

13. Watkins, C.E., Runyan, H.L., and Woolston, D.S., "On the Kernel Function of the Integral Equation Relating the Lift and Downwash Distributions on Oscillating Surfaces in Subsonic Flow", NACA Report No. 1234, 1955.

14. Cunningham, A.M., "A Collocation Method for Predicting Oscillatory Subsonic Pressure Distributions in Interfering Parallel Lifting Surfaces", AIAA Paper No. 71-329, 1971.

15. Ruo, S.Y., Yates E.C., Jr., and Theisen, J.G., "Calculation of Unsteady Transonic Aerodynamics for Oscillating Wings with Thickness", AIAA Paper No. 73-316, 1973.

16. Rodemich, E.R., and Andrew, L.V., "Unsteady Aerodynamics for Advanced Configurations, Part II - A Transonic Box Method for Planar Lifting Surfaces", Air Force Flight Dynamics Laboratory Report No. FDL-TDR-152, Part II, 1965.

17. Garrick, I.E., "Nonsteady Wing Characteristics", High Speed Aerodynamics and Jet Propulsion, Vol. VII - Aerodynamic Components of Aircraft at High Speeds, (A.F. Donovan and H.R. Lawrence, Editors) Princeton University Press, 1957, pp. 658-778.

18. Zienkiewicz, O.C., and Cheng, Y.K., The Finite Element Method in Structural and Continuum Mechanics, McGraw-Hill, 1967.

19. Oden, J.T., "A General Theory of Finite Elements - Parts I and II", International Journal of Numerical Methods in Engineering, Vol. 1, 1969.

20. Allred, J.C., and Newhouse, A., J. Acoust. Soc. Amer. 30, pp 1-3, 1958.

21. Allred, J.C., and Newhouse, A., J. Acoust. Soc. Amer. 30, pp 903-904, 1958.

22. Hunt, F.V., J. Acoust. Soc. Amer. 36, pp 556-564, 1964.

23. Schroeder, M.R., J. Acoust. Soc. Amer. 45. pp.1077-1088, 1969.

24. Schroeder, M.R., and Kuttruff, K.H., J. Acoust. Soc. Amer. 34, pp 76-80, 1962.

25. Schroeder, M.R., J. Acoust. Soc. Amer. 46, p 1819, 1962.

26. Schroeder, M.R., J. Acoust. Soc. Amer. 46, pp 277-283, 1969.

27. Schroeder, M.R., J. Acoust. Soc. Amer. 47, 424-431, 1970.

28. Haviland, J.K., and Thanedar, B.D., "Theoretical Study of Reactive Fluid Flow in Heterogeneous Combustion Processes-Supplement I", University of Virginia, Research Laboratories for the Engineering Sciences, Report No. AEEP- 4007-110-71U, 1971.

29. Haviland, J.K., "The Solution of Two Molecular Flow Problems by the Monte Carlo Method", Methods in Computational Physics, Vol. 4, Applications in Hydrodynamics, (Ed. by Berni Alder), Academic Press, pp 164-165, 1965.

30. Mintzer, D., J. Acoust. Soc. Amer., 22, pp 341-352, 1950.